Toxicology Reports 8 (2021) 920–937

Contents lists available at ScienceDirect

Toxicology Reports

journal homepage: www.elsevier.com/locate/toxrep

Short-term whole body cigarette smoke exposure induces regional differences in cellular response in the mouse larynx

Meena Easwaran, Joshua D. Martinez, Daniel J. Ramirez, Phillip A. Gall, Elizabeth Erickson-DiRenzo *

Department of Otolaryngology-Head and Neck Surgery, Stanford University School of Medicine, Stanford, CA, USA

ARTICLE INFO

Edited by Dr. A.M. Tsatsaka

Keywords:
Cigarette smoke
Murine larynx
Cell proliferation
Cell death
Surface topography
Mucus production

ABSTRACT

The larynx is an essential organ in the respiratory tract and necessary for airway protection, respiration, and phonation. Cigarette smoking is a significant risk factor associated with benign and malignant laryngeal diseases. Despite this association, the underlying mechanisms by which cigarette smoke (CS) drives disease development are not well elucidated. In the current study, we developed a short-term murine whole body inhalation model to evaluate the first CS-induced cellular responses in the glottic [i.e. vocal fold (VF)] and subglottic regions of the larynx. Specifically, we investigated epithelial cell proliferation, cell death, surface topography, and mucus production, at various time points (1 day, 5 days, 10 days) after ~ 2 h exposure to 3R4F cigarettes (Delivered dose: 5.6968 mg/kg per cigarette) and following cessation for 5 days after a 5 day CS exposure (CSE). CSE elevated levels of BrdU labeled proliferative cells and p63 labeled epithelial basal cells on day 1 in the VF. CSE increased proliferative cells in the subglottis at days 5, 10 and following cessation in the subglottis. Cleaved caspase-3 apoptotic activity was absent in VF at all time points and increased at day 1 in the subglottis. Evaluation of the VF surface by scanning electron microscopy (SEM) revealed significant epithelial microprojection damage at day 10 and early signs of necrosis at days 5 and 10 post-CSE. SEM visualizations additionally indicated the presence of deformed cilia at days 5 and 10 after CSE and post-cessation in the respiratory epithelium lined subglottis. In terms of mucin content, the impact of short-term CSE was observed only at day 10, with decreasing acidic mucin levels and increasing neutral mucin levels. Overall, these findings reveal regional differences in murine laryngeal cellular responses following short-term CSE and provide insight into potential mechanisms underlying CS-induced laryngeal disease development.

1. Introduction

Cigarette smoking is the leading preventable cause of death in the United States [1]. Long-term inhalation or exposure to cigarette smoke (CS) affects multiple organ sites within the body and leads to a multitude of benign and malignant diseases. This is not surprising as the smoke produced from burning a cigarette contains more than 7000 harmful toxicants in both gaseous and particulate phases, including at least 70 carcinogenic substances [2,3]. The respiratory tract is a primary target for such toxicants [4]. Despite decades of research, pathogenetic

Abbreviations: AB/PAS, Alcian blue/Periodic acid Schiff; BLOQ, below limits of quantitation; BrdU, 5-bromo-2′-deoxyuridine; BSA, bovine serum albumin; CBF, ciliary beat frequency; CC3, cleaved caspase-3; CO, Carbon monoxide; CS, cigarette smoke; CSE, cigarette smoke exposure; DAB, 3,3′-diaminobenzidine; FTC/ISO, Federal Trade Commission/International Standard Organization; GSD, geometric standard deviation; H&E, Hematoxylin and Eosin; HIER, heat-induced antigen retrieval; HPF, high power field; MCC, mucociliary clearance; MMAD, Mass median aerodynamic diameter; NMR, nicotine metabolite ratio; OECD, organization for economic co-operation and development; PAHs, polycyclic aromatic hydrocarbons; RE, respiratory epithelium; REV, reversibility; ROS, reactive oxygen species; SCIREQ, Scientific Respiratory Equipment Inc; SEM, scanning electron microscopy; SSE, stratified squamous epithelium; SWGTOX, Scientific Working Group for Forensic Toxicology; TBST, tris-buffered saline-tween 20; TPM, total particulate matter; TSNA, tobacco-specific nitrosamines; UPLC-MS/MS, ultra-performance liquid chromatography-tandem mass spectrometer; VF, vocal fold; VSC, veterinary service center.

* Corresponding author at: Division of Laryngology, Department of Otolaryngology-Head & Neck Surgery, Stanford University School of Medicine, 801 Welch Road, Stanford, CA, 94305-5739, USA.

E-mail addresses: meenae@stanford.edu (M. Easwaran), joshua.martinez@stanford.edu (J.D. Martinez), dajorami@ucsc.edu (D.J. Ramirez), philgall@stanford.edu (P.A. Gall), edirenzo@stanford.edu (E. Erickson-DiRenzo).

https://doi.org/10.1016/j.toxrep.2021.04.007
Received 10 December 2020; Received in revised form 11 April 2021; Accepted 16 April 2021
Available online 19 April 2021

mechanisms related to short- and long-term CS-induced respiratory tract perturbations are still not fully understood.

The larynx is a hollow, tubular-shaped organ situated in the upper respiratory tract [5]. It provides protection to the lower airways and is essential for breathing, coughing, swallowing, and in humans, voice production [6,7]. Despite these critical functions, the larynx is an understudied region within the upper respiratory tract. Anatomically, the larynx can be divided into three regions: supraglottis, glottis (i.e., vocal folds), and subglottis. The surfaces of the larynx, particularly the glottic area, are susceptible sites for deposition of the inhaled toxicants associated with CS [8,9]. Inhalation of CS is the primary risk factor for the development of glottic cancer [10]. Also, CS is one of the most common causes of chronic vocal fold (VF) inflammation (i.e. chronic laryngitis) [11]. The pathophysiological mechanisms by which smoking causes laryngeal diseases have not been well elucidated.

The epithelium of the respiratory tract is the first surface to come in contact with CS and it plays an essential protective role by providing a physical barrier. The larynx is lined by two types of epithelial cells. The glottic, or VF region is lined by a stratified squamous epithelium (SSE) [12]. The supraglottic and subglottic regions are lined by ciliated pseudostratified columnar epithelium (i.e., respiratory epithelium [RE]) with integrated mucus-producing goblet cells and underlying submucosal glands. Both epithelial cell types are derived from a population of cuboidal-shaped basal stem/progenitor cells [13,14]. The basal cells are located just above the basement membrane and express cytokeratins 5 and 14 and transcription factor TP63 (p63). The protective capacity of the laryngeal epithelium may be compromised due to repeated insults from CS and likely plays a major role in the pathogenesis of CS-induced laryngeal diseases.

In healthy epithelium, cell proliferation, the process whereby cells replicate themselves by growing and then dividing into two equal copies, is tightly regulated and essential for normal epithelial turnover [15]. However, CS contains a multitude of toxicants [16]. Toxicants like acrolein [17], ammonia [18,19], crotonaldehyde [20], and formaldehyde [21] can alter cell proliferation upon acute inhalation in the rodent respiratory tract [22–25]. Specifically, increased cell proliferation, either by an increased rate of proliferation and/or an increase in overall cell number (hyperplasia), may occur in response to CS exposure (CSE). Increased cell proliferation may be an adaptive response to an injurious substance [26]. However, an important feature of laryngeal malignant transformation is the large number and high proliferation rate of dividing cells [27]. While CS has been shown to induce laryngeal epithelial hyperplasia [28,29], very few studies have directly investigated proliferating cells in response to CSE. One technique for investigating proliferating cells is through the use of BrdU (5-Bromo-2′-deoxyuridine), an analog of thymidine nucleotide base. BrdU is a cell cycle marker, which can specifically identify proliferating cells in the "S" or division phase of the cycle [30]. Immunohistochemical BrdU labeling indices have been used to directly measure cell proliferation in urothelial, pulmonary, vascular systems in response to short-term CS, oral nicotine delivery, and other environmental toxicant exposures [31–34].

Proliferative changes may also be observed in the mucus-producing cells of the laryngeal subglottic region. Mucus is the thin layer of fluid that covers the epithelial surface and is the first line of defense in the larynx [35]. As part of the mucociliary clearance process, mucus traps inhaled toxicants as present in CS for clearance by ciliary movement from the larynx through coughing or swallowing [36]. However, trapped toxicants may alter mucus-producing cell structure and function, leading to defective mucus barrier. CS induces hyperplasia or hypertrophy of mucus-producing cells in the lung, bronchial, and nasal airway tissue [37–39]. There is some limited evidence to suggest that CS also induces subglandular hypertrophy and mucus hypersecretion in the larynx [40,41]. However, BrdU labeled cell proliferation in these structures has not been evaluated. It is essential to understand the importance of CS-induced proliferative changes in the mucus-producing cells of the larynx in conjunction with studying its importance in the laryngeal VF epithelium. Furthermore, mucus is histochemically classified as acidic or neutral. Acidic mucus has a negative charge due to presence of carboxyl or sulphonic groups whereas neutral mucus has no charged groups. Both types of mucus contribute to its defensive properties including trapping of inhaled particulates and lubrication [42,43]. In other tissues, such as colorectal, alterations in mucus composition are associated with disease states [42,43]. Upon CS inhalation, morphological changes to mucus producing cells may also contribute to shifts in mucus composition in the larynx, ultimately contributing to altered mucosal defense and disease progression.

Under normal conditions, the maintenance of epithelial cell homeostasis involves a tightly regulated balance between cell proliferation and cell death mechanisms. Abnormal conditions like repeated exposures to CS can induce an imbalance between cell proliferation and cell death. Constituents of CS like polycyclic aromatic hydrocarbons (PAHs) and nitrosamines cause direct DNA damage via reactive oxygen species (ROS) production, induction of mutations and DNA adduct formation, thereby contributing to CS-induced cytotoxic responses via apoptosis and/or necrosis [44]. However, there is a risk of abnormal cellular proliferation leading to carcinogenesis, if there is suppression or inactivation of cell death mechanisms through induction of mutations [45,46]. Multiple in vitro studies have reported that CS can induce epithelial cell death depending upon the dose of CSE [47–50].

Cell death in response to CS in the larynx has not been well elucidated. Immunohistochemical evaluation is the primary means to detect CS-induced epithelial cell death [48,51,52]. However, these evaluations may not provide complete insight into CS-induced cytotoxic responses. Scanning electron microscopy (SEM) is a widely used tool to analyze cellular changes at the epithelial level, the first surface exposed to CS inhalation. Previous reports show that cells undergoing CS-induced apoptosis or necrosis can be visually analyzed using SEM [33,51]. Incorporating this procedure in addition to the immunohistological examinations can thus enhance our understanding of CS-induced cytotoxicity in the larynx.

It is essential to understand the underlying pathophysiological mechanisms of laryngeal diseases associated with CS, for better clinical assessments and interventions. It is well established that long-term exposure to CS causes benign and malignant laryngeal disease. However, it is critical to elucidate initial cellular responses to CS within the larynx, to better understand the effects of chronic smoking, since repetitive acute smoke effects may cumulate and ultimately lead to tissue damage associated with the disease [53]. No known studies have investigated the short-term effects of smoking on the laryngeal mucosa. The objective of this study was to investigate key epithelial and subglandular changes of murine laryngeal mucosa upon short-term CSE. Specifically, we evaluated the early effects of CSE on cellular proliferation, cytotoxicity, and mucus production within the glottic and subglottic regions of the murine larynx. We also assessed the extent of smoking by analyzing levels of nicotine and its metabolites in the urine of mice exposed to short-term CS.

2. Materials and methods

2.1. Animals

All procedures were performed in conformance with the approved protocol guidelines by the Stanford University Institutional Animal Care and Use Committee. Male C57BL/6J mice, 8–9 weeks old (n = 56), were purchased from Jackson Laboratories (Sacramento, CA, USA). Mice were provided normal chow, water ad libitum, and housed in ventilated cages in a designated room in the Stanford University School of Medicine Veterinary Service Center (VSC). Mice were continuously monitored by laboratory and VSC personnel. The individual weight of mice in each experimental group was measured using a Tanita Small Animal Scale (Model: KD-160), thrice weekly (Monday, Wednesday, and

Friday).

2.2. Experimental design and cigarette smoke exposure

Mice were randomly assigned to CS exposure (CSE), reversibility (REV), and air-exposed control groups. CSE group mice were exposed to CS (~2 h/day- AM/PM, 5 days/week) for 1 day (n = 8), 5 days (n = 8) and 10 days (n = 8). Mice in the REV group (n = 8) were exposed to CS for 5 days and then air-exposed the next 5 days. At all time points, control mice were left exposed to room air in their housing conditions (Fig. 1). In this investigation, we utilized a common reference cigarette, 3R4F Kentucky research cigarettes (Center for Tobacco Reference Products, University of Kentucky, Lexington, KY). This cigarette contains burley, oriental, flue cured and reconstituted tobacco, and designed to be representative of commonly sold American blend cigarettes [54]. CSE and REV group mice were exposed to mainstream CS from 14 cigarettes using the inExpose™ inhalation exposure system (Scientific Respiratory Equipment Inc [SCIREQ], Montreal, QB, Canada). Mice were placed into the whole body chamber of the inExpose™ system (Fig. 2). Separators were used to isolate animals and eliminate the possibility of huddling together, which may impede effective inhalation. Exposure protocols were designed in accordance with the Federal Trade Commission (FTC)/International Standard Organization (ISO 1991) standard of 35 mL puffs of 2 s duration followed by 58 s of fresh air at a rate of 2 L/min, taken once a minute. These protocols were run using the SCIREQ software application Flexiware (v8.0). CS generated was directed into a whole body exposure chamber using pumps mounted on the standard base unit (Fig. 2). The puff count number per cigarette was set to 9 based on the University of Kentucky 3R4F preliminary analysis reports and previous puff count numbers obtained via FTC/ISO methods [55–57]. Based on these exposure parameters, the time for exposing mice to 14, 3R4F cigarettes per day was approximately 2 h 6 min (126 min per day) (Supplementary Data S2). Delivered dose was 5.6968 mg/kg per cigarette and 79.755 mg/kg for 14 cigarettes (per day) (Supplementary Data S1). The average TPM concentrations during exposure was computed as ~621 mg/m^3, which is considered high dosing CS (Supplementary Data S2).

2.3. BrdU administration, animal euthanasia, and sample collection

Mice in the CSE, REV, and control groups were administered 5-Bromo-2′-deoxyuridine, BrdU (100 mg/kg body weight; ab142567, Abcam, CA, USA) via intraperitoneal injections, immediately following the final CS or air exposure (Fig. 1). Two hours after BrdU administration, mice were euthanized by cervical dislocation under deep anesthesia by isoflurane (Fig. 1). Urine was collected by terminal bladder puncture and stored at −80 °C until analysis for tobacco biomarkers. Larynges were harvested and processed for histomorphometric analysis, immunostaining, and SEM (Fig. 1).

2.4. General assessment of whole body CSE using urinary biomarkers

Whole body CS inhalation exposure was evaluated by analysis of two major nicotine metabolites, cotinine and trans-3′-hydroxycotinine in the mice urine samples. This analysis was performed by Nicotine and Tobacco Product Assessment Resource (NicoTAR) at Roswell Park Comprehensive Cancer Center (Buffalo, NY, US). Nicotine metabolites were quantified using ultra-performance liquid chromatography coupled with tandem mass spectrometry (UPLC-MS/MS). Below Limits of Quantitation (BLOQ) for cotinine and trans-3′-hydroxycotininee was set to <1.0 ng/mL and <2.0 ng/mL respectively. The analysis was performed in control, 5 day REV, 5, and 10 days CSE groups. Method calibration, validation, and concentration determinations were conducted as per the Scientific Working Group for Forensic Toxicology (SWGTOX) Standard Practices for Method Validation in Forensic Toxicology (SWGTOX, 2013). The rate of nicotine metabolism (NMR) was also evaluated as a measure of the ratio between total urine trans-3′-hydroxycotinine levels to total urine cotinine levels.

2.5. Histomorphometric analysis of laryngeal mucosa

Larynges harvested from the CSE, REV, and control groups were fixed in 4% paraformaldehyde overnight at 4 °C, transferred to 70% ethanol, and sent to HistoWiz, Inc. (http://www.histowiz.com; Brooklyn, NY) for tissue processing, paraffin embedding, and microtomy per established methods [58,59]. A small portion of trachea was left on the larynx as an anatomical landmark for orientation during paraffin embedding. Post fixation, the larynges were embedded in preparation for coronal sectioning such that the anterior region of the larynx with visible tracheal rings is towards the face of the paraffin block (Supplementary Fig. 1). Paraffin blocks were trimmed until the VF region appeared along with complete separation of the airway lumen between the left and right regions of the larynx (e.g., slide 6 onwards in the Supplementary Fig. 1). Serial laryngeal coronal sections (5 μm) were then obtained from paraffin blocks across all time points. These sections included vocal folds/glottis, subglottic mucus containing glandular regions, thyroid cartilage, cricoid cartilage and tracheal rings (Supplementary Fig. 2). Sections were stained with Hematoxylin and Eosin (H&E) and Alcian blue/Periodic Acid Schiff (AB/PAS) for assessment of VF epithelial thickness and subglottic glandular area and composition, respectively.

2.5.1. Measurement of vocal fold (VF) epithelial thickness

Right and left VF epithelial thickness was measured by analysis of digital images obtained from H&E stained slides at 20x magnification. The VF epithelium was traced along the mid-membranous region (~340 μm in length) using the pen tool on the digital pathology software Aperio ImageScope v.12.3.2.8013 (Leica Biosystems, Germany). The distance measurement tool was then applied to these traced regions and an average thickness between five different points was computed.

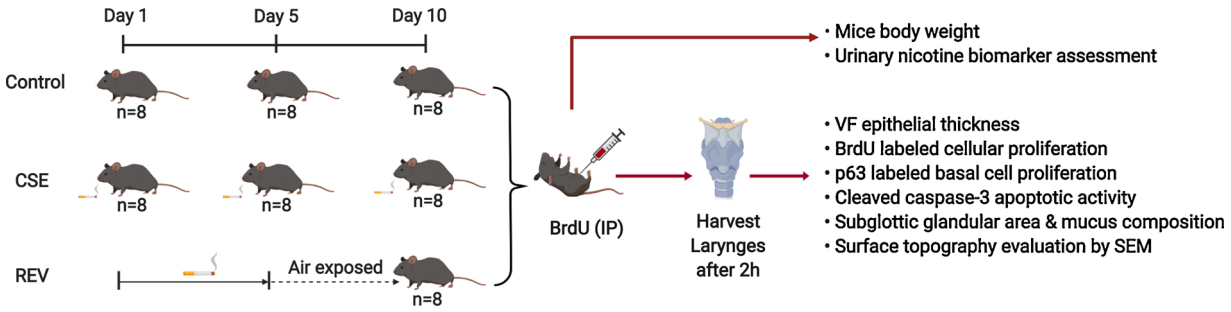

Fig. 1. Experimental design. Adult male C57BL/6J were exposed to room air conditions (Control) and CS for 1, 5, and 10 days. Mice in the REV group were exposed to CS for 5 days followed by room air exposure for an additional 5 days. All CS exposures were performed ~2 h/day, 5 days/week. At the end of exposures at each time point, mice were euthanized 2 h after BrdU intraperitoneal administration, and larynges were harvested for cellular analyses.

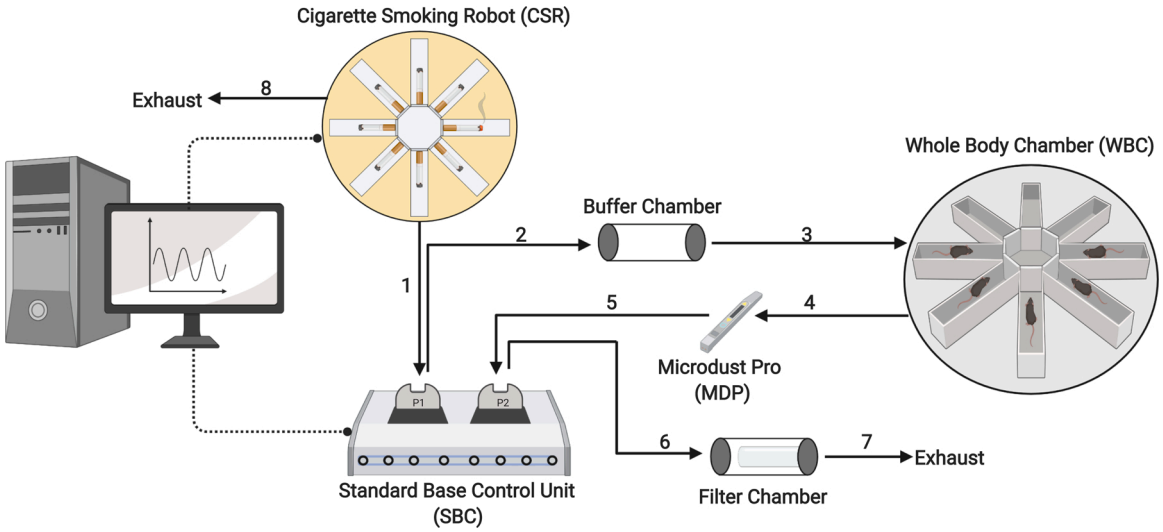

Fig. 2. Adapted schematic illustration of mainstream CSE using inExpose™ inhalation exposure system. 3R4F cigarettes placed in the cigarette smoking robot (CSR) carousel are automatically lit, upon activation of the system. CS from CSR is drawn (1) by pump 1 - P1 on the standard base control unit (SBC) and delivered to mice in the whole-body chamber (WBC) via buffer chamber (2 & 3). Remnant smoke post inhalation in the chamber is drawn by pump 2 -P2 and it passes via a probe, Microdust Pro (MDP) for real-time particulate matter monitoring (4 & 5). Smoke is then passed into a paper filter containing chamber (6) before finally exhausting out of the system (7). Excess smoke within CSR is also exhausted (8). Dotted lines with black circular heads at the end indicate connecting cables. Actual CSR can hold up to 24 cigarettes and WBC can house 16 mice in total.

2.5.2. Analysis of total subglottic glandular area and mucus composition

The digital images of AB/PAS stained slides were utilized to measure the subglottic glandular area and mucus composition by Fiji (derivative of ImageJ; NIH). For the subglottic glandular area analysis, the glandular regions on the right and left side were first traced manually with the polygon tool at 10x magnification. The area measurements were then set to include glands sized more than 100 μm^2. To quantify mucus composition, the stain vectors in the color deconvolution tool were applied to obtain separate images of the AB stained acidic mucins (blue) and PAS stained neutral mucins (purple/magenta). Subsequent procedures similar to the total subglandular area analysis were followed to evaluate area stained for acidic and neutral mucins.

2.6. Immunohistochemical assessment of cellular proliferation by BrdU labeling

Standard immunohistochemistry procedures to stain BrdU were performed by HistoWiz, Inc (histowiz.com). Positive reactions resulted in brown nuclear staining using 3,3′-Diaminobenzidine (DAB) as a substrate. The number of BrdU positive cells were counted in the VF and subglottic region. Positive cells were counted on 20x images of the left and right vocal folds. For subglottic BrdU analysis, areas were randomly selected at 10x along a fixed length of 700 μm in epithelial and subepithelial regions on both the right and left sides. The counts were performed at 40x within ten high power fields (HPFs) in this area. For both the VF and subglottic regions, the counter tool on Aperio ImageScope v.12.3.2.8013 (Leica Biosystems, Germany) was used to quantify the number of labeled cells.

2.7. Detection of basal cells by immunofluorescence

Routine immunofluorescence protocol was followed to stain VF basal cells with p63 (1:100; CM 163 A, Biocare Medical LLC, CA, USA). Unstained slides were deparaffinized in xylene and rehydrated in an ethanol series. Heat-induced antigen retrieval (HIER) was performed with 1X Citrate buffer (ph. 6.0; C999, Sigma, USA) at 121 °C for 15 min followed by 1 h of cooling at room temperature. The slides were blocked with a blocking buffer (1% Bovine serum albumin [BSA], 0.2% Triton-X-100, 10% Sodium Azide, 2% Donkey serum) for 1 h at room temperature. The primary antibody diluted in a solution containing 0.5% BSA, 0.2% Triton-X-100 and 10% Sodium Azide, was applied to the slides and left to incubate overnight at 4 °C in a humidified chamber. The slides were then incubated for 1 h after the application of donkey-anti-mouse secondary antibody conjugated to Alexa Fluor 647 (1:500; A-31571, Invitrogen, CA, USA). The slides were washed with 1X Tris-buffered saline-tween 20 (TBST) solution and treated with Hoechst nuclear counterstain (33258, Sigma, USA). The slides were then mounted with Dako aqueous mounting medium (10131720, Agilent Dako, CA, USA). The slides were viewed, and images were acquired at 20x by Axioimager microscope (Zeiss). p63 positive basal cells were counted in the right and left mid-membranous region of the VF across a fixed length of 300 μm using the counter tool in Fiji.

2.8. Evaluation of apoptosis by immunohistochemistry

To detect apoptosis, the slides were immunohistochemically stained with antibodies against cleaved caspase-3 (CC3) using the ImmPRESS Excel Amplified HRP Polymer kit for anti-Rabbit IgG's (MP-7601, Vector laboratories, CA, USA). Slides were deparaffinized, rehydrated, and subjected to HIER. The sections were blocked with ready to use 2.5% normal horse serum provided in the kit for 20 min and incubated with primary anti-CC3 (1:500; 9664 T, Cell Signaling Technology, MA, USA) at 4 °C, overnight. The slides were counterstained with Hematoxylin QS (H-3404, Vector Laboratories, CA, USA) for 45 s, dehydrated, and mounted with glass coverslips. Images of CC3 stained slides were obtained at 40x using the Axioimager microscope (Zeiss). CC3 positive cells were counted along the entire mid- membranous VF region. In the right and left subglottic regions, a subset of five different 100 × 100 μm sized regions were randomly selected across the entire subglottis and counted along the epithelium and glandular region.

2.9. Surface topography evaluation of the VF by scanning electron microscopy (SEM)

Routine methods were used to process tissue for SEM as described previously [60]. Briefly, larynges were fixed (2.5% glutaraldehyde, 4% formaldehyde, 0.05 mM Hepes Buffer pH 7.2, 2 mM CaCl2, 0.5 mM MgCl2, 0.9% NaCl) and dehydrated. Following dehydration, samples

were split longitudinally to reveal the VF surface (right and left) and then underwent critical point drying. Following the critical drying step, samples were mounted, and sputter coated with Au/Pd (gold/-palladium; 60:40 ratio). Samples were imaged by FEI Strata 235 DB DualBeam FIB/SEM and images were obtained at 5 - 25kx.

Damage to the VF surface microprojections was evaluated using standard visual examination [61]. For each group, twenty 2 × 2 μm sized SEM images were randomly selected from the original 25kx images of the right and left vocal folds. Images were presented to three blinded judges who submitted characterizations using the web-based software application Blinder (Solibyte Solutions, Durham, NC; http://blinder.solibytesolutions.com/) to score images based on four categories of damage severity: normal (score 0), mild/minimal (score 1), moderate (score 2) and extensive/severe (score 3). Images were categorized as normal if there was no microprojection damage. Slightly dented and less dense microprojections were classified as mild/minimal damage. The moderate damage category displayed denting or flattening of all microprojections. The extensive/severe damage category was characterized by the destruction of cellular surfaces and the exposed cytoskeleton. Within the software, 50% of SEM images were scored twice (Quality control parameter) to ensure consistent scoring. Images that failed quality control and those which had discrepancies were reclassified by the judges by a consensus rating.

2.10. Statistical analysis

Since analysis was completed manually by an unblinded rater for measurements related to vocal fold epithelial thickness, subglottic glandular area and mucus composition, BrdU labeling, basal cell labeling, and apoptosis, 20% of samples were randomly chosen and reanalyzed by blinded raters for assessment of intra- and inter-rater reliability. For this analysis, two-way mixed-effects, absolute agreement intraclass correlation coefficients (ICC) were performed using SPSS Statistics (Version 26, IBM). Interpretation was as follows: <0.50, poor; between 0.50 and 0.74, fair, between 0.75 and 0.90 good; above 0.90 excellent [62].

All other statistical analyses were performed by using GraphPad Prism version 8.4.2. For comparisons involving two independent groups with a) equal sample sizes, Student's *t*-test was performed and with b) unequal sample sizes, Welch's *t*-test was performed. Microprojection damage data obtained by visual scoring of the right and left vocal folds were analyzed by Kruskal–Wallis test followed by post hoc uncorrected Dunn's test. All other measurements were analyzed by one-way analysis of variance (ANOVA) and post hoc Fisher's Least Significant Difference (LSD) multiple comparison test. Grubb's test was run on the cleaved caspase-3 subglottic dataset to identify and eliminate outliers. Values less than $p \leq 0.05$ were considered significant. All data are represented in figures as means ± standard deviations (SD).

3. Results

3.1. Reliability

Mean estimates along with 95% confidence intervals (CI) are reported for each intra- and inter-rater ICC in Supplementary Table 1. ICCs for intra-rater reliability were between good and excellent. ICCs for inter-rater reliability were also primarily between good and excellent, with only a single ICC (acidic mucin quantification) in the fair range.

3.2. Mice survival and body weight measurements

All the mice survived during the entire duration of smoke exposure. No other health-related issues were reported. At the time of euthanasia, mice exposed to CS exhibited significant body weight decrease at day 5 (Fig. 3A) and day 10 (Fig. 3B) in comparison to their respective control. At the end of 5 days of CSE, the body weight of mice in the 5 day REV group was significantly less than controls (Fig. 3C). However, these mice also exhibited a significant increase in weight post CS cessation (Fig. 3C).

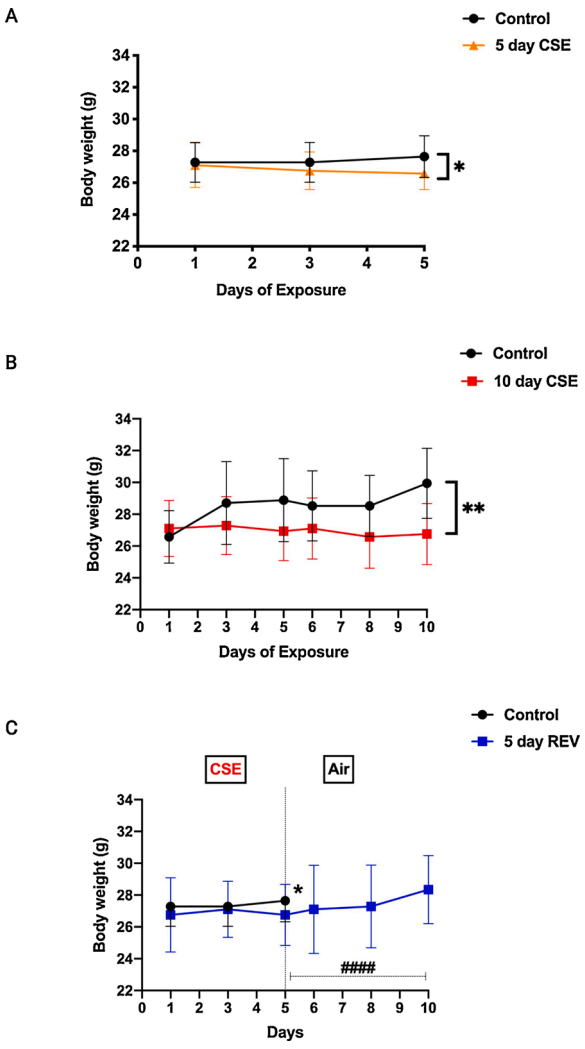

Fig. 3. Body weight measurements. CSE mice exhibit significant weight loss at days 5 (A) and 10 (B). Although, the body weight of mice in the 5 day REV group was significantly lesser than the controls, these mice exhibited a significant body weight gain post CS cessation at day 5 (C). n = 8 in control, 1 day CSE, 5 day CSE, 5 day REV, and 10 day CSE groups. Line graphs show the mean with SD. * $p \leq 0.05$, ** $p \leq 0.01$ and #### $p \leq 0.0001$.

3.3. General assessment of whole body CSE by analysis of urine nicotine biomarker levels

Urine cotinine levels were significantly elevated only at day 5 (Fig. 4A) post-CSE when compared to control, 5 day REV, and 10 day CSE groups. Trans-3′-hydroxycotinine levels were found to be significantly higher on day 5 after CSE (Fig. 4B) in comparison to the control, 5 day REV, and 10 day CSE groups. Mice in 10 day CSE group (Fig. 4B) also have significantly increased levels of trans-3′-hydroxycotinine in urine when compared to control and 5 day REV group mice. NMR was found to be significantly increased after 10 days of CSE (Fig. 4C) in comparison to control, 5 day CSE, and 5 day REV groups. Mice in the 5 day CSE group (Fig. 4C) also had a significantly higher NMR than the control group mice.

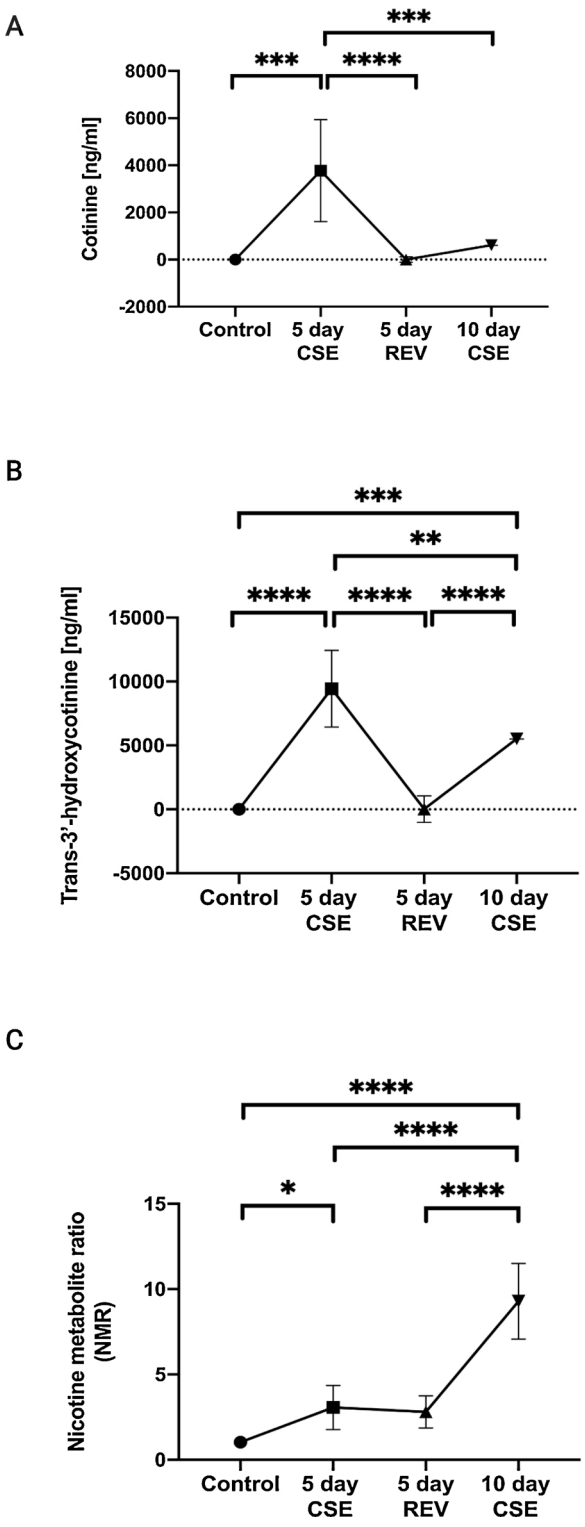

Fig. 4. General assessment of whole body CSE using urinary biomarkers. The amount of urinary cotinine was significantly higher in mice after 5 days of CSE (A) when compared to mice in control, 5 day REV, and 10 day CSE groups. Presence of trans-3′-hydroxycotinine in urine was significant in mice after 5 days and 10 day of CSE (B) when compared to mice in control and 5 day REV groups. Trans-3′-hydroxycotinine levels were significantly higher after 5 days of CSE (B) than 10 days of CSE. Nicotine metabolite ratio (NMR) was significantly increased after 10 days of CSE (C) when compared to control, 5 day CSE, and 5 day REV groups. NMR was also significant at day 5 after CSE (C) in comparison to the control. n = 4 in control, n = 5 in 5 day CSE, 5 day REV, and 10 day CSE groups. Line graphs show the mean with SD. * $p \leq 0.05$, ** $p \leq 0.01$, *** $p \leq 0.001$ and **** $p \leq 0.0001$.

3.4. Histomorphometric analysis of laryngeal mucosa

Evaluation of VF epithelial thickness in the H&E slides revealed that CSE had no significant effect in altering the thickness at all time points and also under reversible conditions (Fig.5A-H). Assessment of mucus-producing glandular area in the AB/PAS slides in the subglottic region indicated that CSE had no major impact. The subglottic glandular area was not significantly increased in the CS exposed groups at all time points and in the 5 day REV group (Fig. 6A-H). Area of AB-positive acidic and PAS-positive neutral mucin levels did not change in the CSE group at days 1 and 5 and the 5 day REV group (Fig. 7D, E). Acidic mucins significantly decreased in the CSE group on day 10 (Fig. 7F). Neutral mucin levels were significantly elevated after 10 days of CSE (Fig. 7F).

3.5. Cell proliferation by BrdU labeling

BrdU labeled cells were significantly elevated only after 1 day of CSE (Fig. 8B, F) in the vocal folds. Proliferative BrdU labeled cells remained unaltered in the 5 day CSE (Fig. 8C, G), 10 day CSE (Fig. 8E, H) and 5 day REV groups (Fig. 8D, G) in comparison to the controls (Fig. 8A). In the subglandular regions, proliferative cells labeled by BrdU had significantly increased after day 5 (Fig. 9C, G) and day 10 of CSE (Fig. 9E, H). Mice in the 5 day REV group (Fig. 9D, G) also had a significant increase in BrdU positive cells when compared to the controls (Fig. 9A).

3.6. VF basal cell proliferation

CS exposed mice showed elevated numbers of p63 positive basal cells at day 1 (Fig. 10B, F) in the vocal folds. Basal cell population remained comparable to the controls (Fig. 10A) in the 5 day CSE (Fig. 10C, G), 10 day CSE (Fig. 10E, H) and 5 day REV (Fig. 10D, G) groups.

3.7. Immunohistochemical analysis of CC3 labeled apoptotic cells

VF regions did not exhibit any significant CC3 levels in the mice exposed to CS at all time points and also in the mice under reversibility conditions (Fig. 11A-H). CC3 positive cells were significantly increased in the subglottis, only on day 1 after CSE (Fig. 12B, F). Mice in 5 day CSE (Fig. 12C, G), 10 day CSE (Fig. 12E, H), and 5 day REV (Fig. 12D, G) groups did not have any significant levels of CC3 positive cells.

3.8. Scanning electron microscopy

3.8.1. Visual scoring of VF epithelial surface microprojections

Significant damage to the VF microprojections was observed only in the mice in the 10 day CSE group (Fig. 13E, J, K) in comparison to the mice in the control (Fig. 13A, F, K) and 1 day CSE group (Fig. 13B, G, K). Visual examination of the right and left vocal folds indicated that CS causes moderate to extensive (score 2–3) damage to the VF after 10 days of CSE (Fig. 13K).

3.8.2. Other morphological observations in the laryngeal mucosa

Epithelial sloughing/exfoliation and ulceration associated with necrosis were seen in the SEM images of the VF regions after 5 and 10 days of CSE, respectively (Fig. 13C, E). The presence of compound cilia was observed in the laryngeal regions lined by RE, after 5 and 10 days after CSE (Fig. 14B, C). In the 5 day REV group (Fig. 14D), damaged ciliary surfaces were discernible from the normal ciliary surfaces. Cellular surface blistering (rounded) accompanied by the ciliary loss was predominantly seen along this epithelium at day 10 post CSE (Fig. 14C, E).

4. Discussion

Cigarette smoking is a major risk factor for the development of benign and malignant laryngeal diseases like chronic laryngitis, Reinke's edema, laryngeal leukoplakia, and laryngeal cancer. In order to

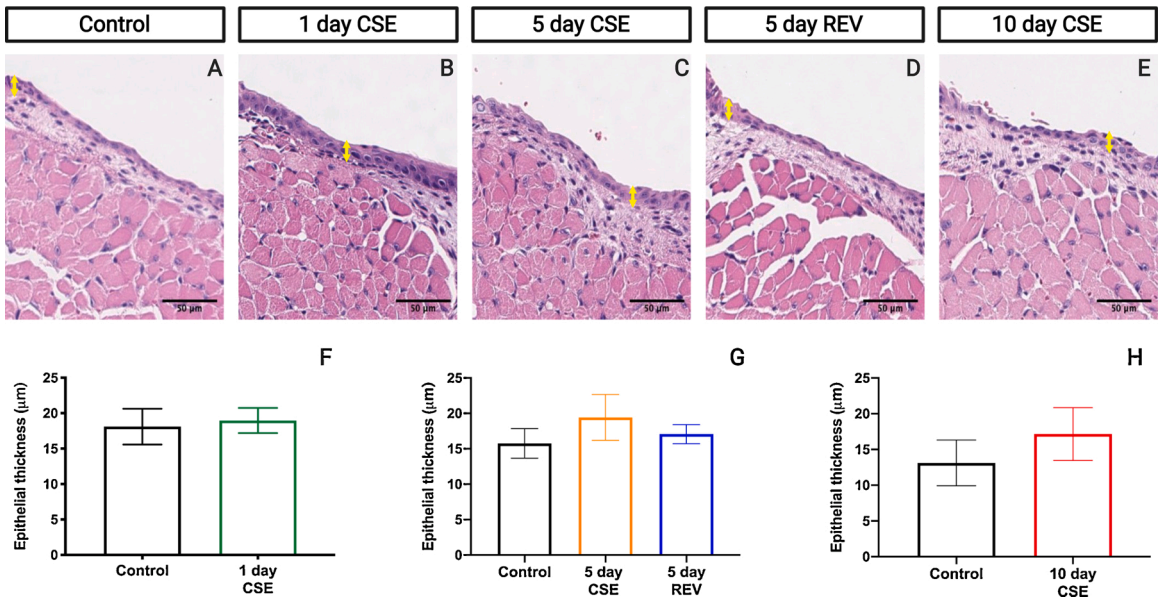

Fig. 5. VF epithelial thickness. CSE did not alter VF epithelial thickness after 1 day of CSE (B, F), 5 days of CSE (C, G), and 10 days of CSE (E, H) when compared to control (A). No major alterations were seen in the 5 day REV group (D, G). At day 1, n = 4 in control and n = 3 in CSE groups. At day 5, n = 5 in control and n = 4 in CSE groups. At day 10, n = 4 in control and n = 5 in CSE groups. n = 5 in 5 day REV group. Yellow double-headed arrows indicate VF epithelial thickness. H&E stained images are at a magnification of 20x. Bar graphs show the mean with SD.

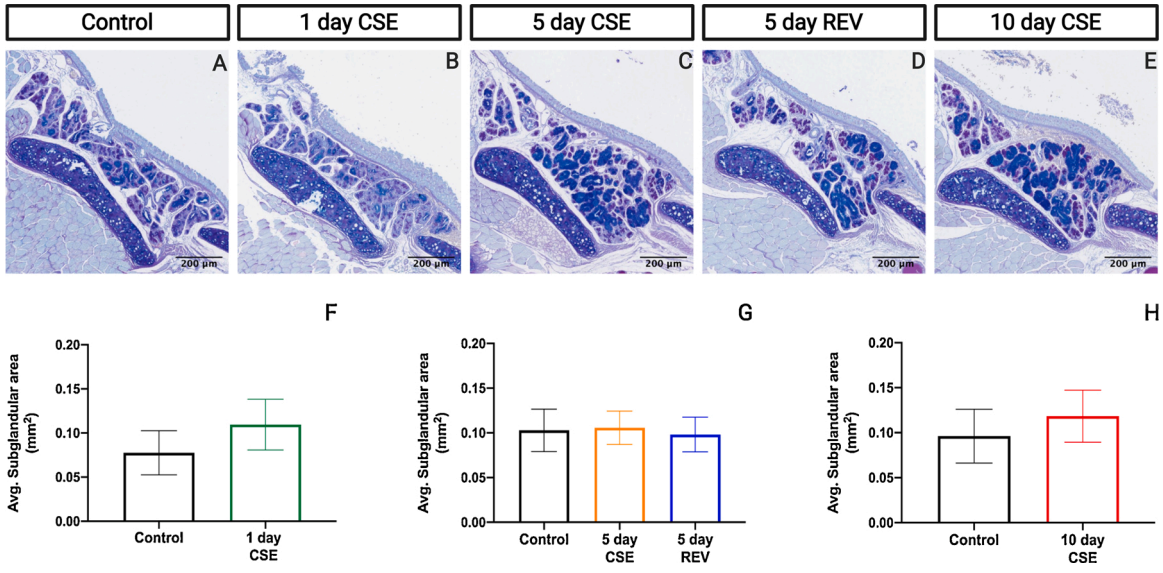

Fig. 6. Total subglottic glandular area. Subglottic glandular regions did not exhibit a significant increase in the area upon CSE at day 1 (B, F), day 5 (C, G) and day 10 (E, H) when compared to the control (A). Mice in the 5 day REV (D, G) group did not show an increase. At day 1, n = 4 in control and CSE groups. At day 5 and day 10, n = 6 in control and CSE groups. n = 6 in the 5 day REV group. AB/PAS stained images are at a magnification of 8x. Bar graphs show the mean with SD.

achieve better understanding of the effects of CS, it is essential to elucidate the cellular events leading up to these disease conditions within a naive larynx. In this study, we exposed mice to short-term, mainstream whole body CS in order to elucidate early cellular responses in the larynx. Results demonstrate that short-term CSE alters cell proliferation, cell death, cell surface topography, and mucin dynamics in different regions of the laryngeal mucosa at varying measured time points. This study's outcome is also indicative of altered rates of nicotine metabolism upon whole body exposure.

CS inhalation studies evaluating the larynx have been conducted previously in rats, hamsters, pigs and guinea pigs [29,40,63,64]. This is not surprising given their larger larynx size, which facilitates post-harvest tissue processing. We selected the mouse for this foundational investigation. Despite being smaller, mice can serve as a strong preclinical model to study CS-induced laryngeal diseases as the larynx is structurally similar to humans [65]. In addition, given the relative ease to genetically engineer mice, in the future, specific mechanisms underlying CS-induced laryngeal disease can be identified and translated into early clinical studies to improve future therapeutic interventions. Mice models have been extensively used to evaluate CS-induced injuries in other airway regions as well [66,67]. We have also been able to successfully induce pathological changes in CS exposed murine larynx [68].

Often inhalation toxicology exposure regimens occur for 6 h/day based on the guidelines published by the Organisation for Economic Co-operation and Development (OECD) for subacute (4 weeks) [69] or

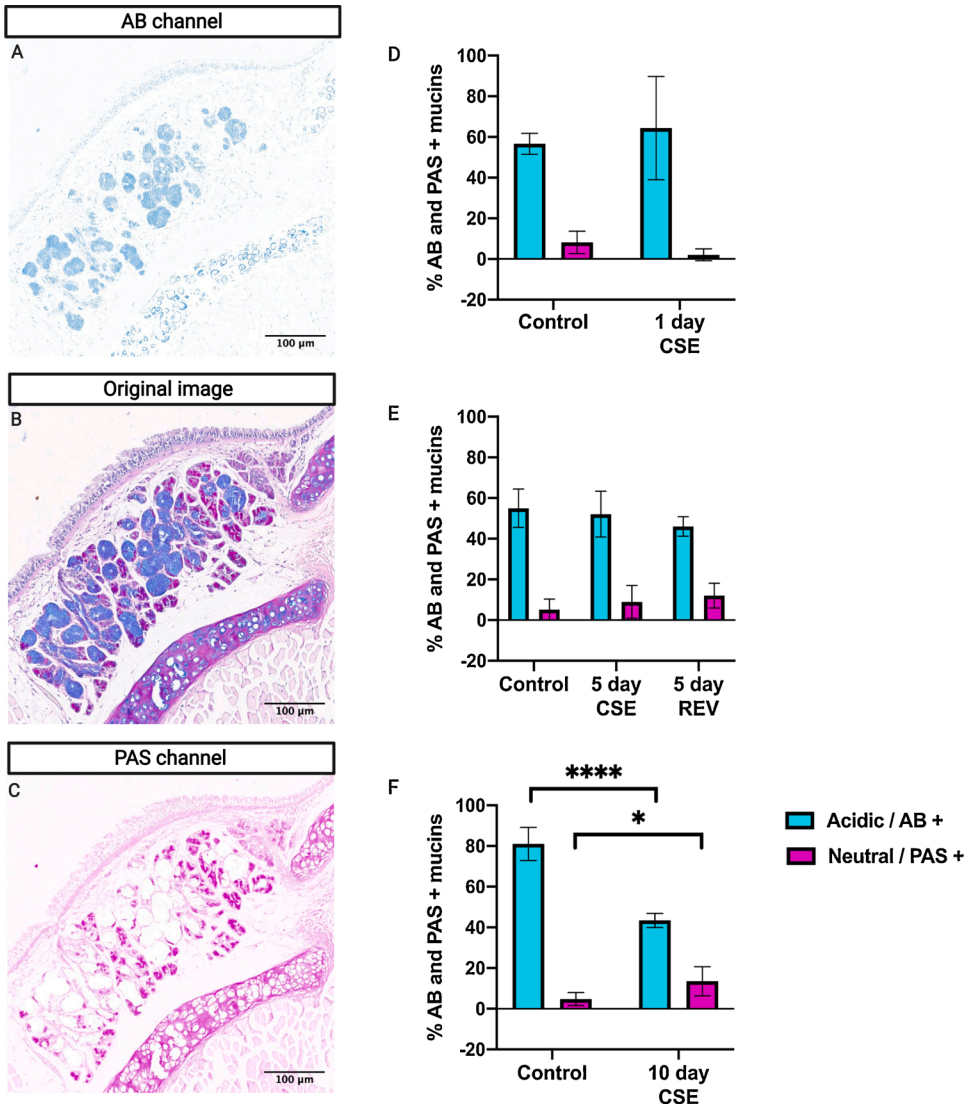

Fig. 7. Mucus composition in the subglottic glandular area. Original AB/PAS stained images (B) were filtered into Alcian blue (A) and Periodic acid schiff (C) channels. Acidic and neutral mucins levels remained unaltered in 1 day CSE (D), 5 day CSE (E), and 5 day REV groups (E). The percentage area of acidic mucins decreased significantly, and the percentage area of neutral mucins increased significantly only after 10 days of CSE (F). At day 1, n = 4 in control and CSE groups. At day 5 and day 10, n = 6 in control and CSE groups. n = 6 in the 5 day REV group. Images are at a magnification of 10x. Bar graphs show the mean with SD. * $p \leq 0.05$, and **** $p \leq 0.0001$.

subchronic (13 weeks) [70] conditions, with the preferred mode of exposure being nose-only. CS-induced lesions in rat larynges and other parts of the respiratory tract have been demonstrated using these OECD guidelines [71–73]. In the current study, mice underwent short-term, whole body daily exposure to mainstream CS for ~2 h/day. Firstly, we recognize that nose-only exposure is a more direct route of targeting the respiratory tract via inhalation. However, in comparison to whole body exposure, nose-only exposure can cause additional stress to rodents due to physical restraints and increased animal handling [74]. Secondly, in terms of exposure regimen, recent studies have demonstrated that exposure regimens < 6 h/day is sufficient to cause histopathological changes within the larynx [68,75,76]. In fact, a recent CSE study demonstrated that 2 h/day exposure to CS for 15 days is sufficient to study the effects on the respiratory tract, including the larynx [77]. Apart from the duration of exposures, the severity of toxicity and these biological responses is also governed by another important factor, exposure concentration.

The fundamental rule of inhalation toxicology, Haber's law postulates that intensity of the toxic response is dependent on total exposure dose i.e., the product of the concentration of inhaled toxicant and time of exposure produces a constant toxic effect (c x t = k) [78,79]. Based on this law, high concentration short-term exposures can result in comparable biological responses to low concentration long-term exposures [80]. Recent studies have evaluated these biological responses by testing various exposure regimens with modified exposure time (~1–6 hours per day) and concentration (~50–800 µg/L) over 2 weeks or 13 weeks of CS exposure [75,76]. These studies have specifically found that histopathological changes occur in the upper airways (nose, larynx, and trachea) irrespective of exposure time and CS concentration. Historically, studies in the larynx have been conducted to evaluate cumulative effects of CS-induced toxicity under pre-chronic and chronic conditions [29,63]. However, based on the equivalent biological response/exposure dosimetry predictions derived from Haber's law, we hypothesized that short-term CS would cause early lesions that would help us understand CS-induced laryngeal disease onset and progression. Hence, we evaluated CS-induced responses by opting for a high concentration short-term CSE regimen in this study. Specifically, the mice were exposed to high concentrations of mainstream CS (621 mg/m^3 TPM) during the ~2 h exposure period, which is similar to other studies conducted in mice [81] and rats [82].

The extent of smoking is estimated by analyzing levels of nicotine and its metabolites. We analyzed two major nicotine metabolites, cotinine and trans-3′-hydroxycotinine, in the urine of mice exposed to CS via whole body exposure. We also computed the nicotine metabolite ratio (NMR: a ratio of trans-3′-hydroxycotinine to cotinine) as a sensitive measure for determining the level of CS consumption [83]. Cotinine levels were significantly elevated at day 5 of CSE, but comparable to controls at day 10. In contrast, mice in the 5 and 10 day CSE group had

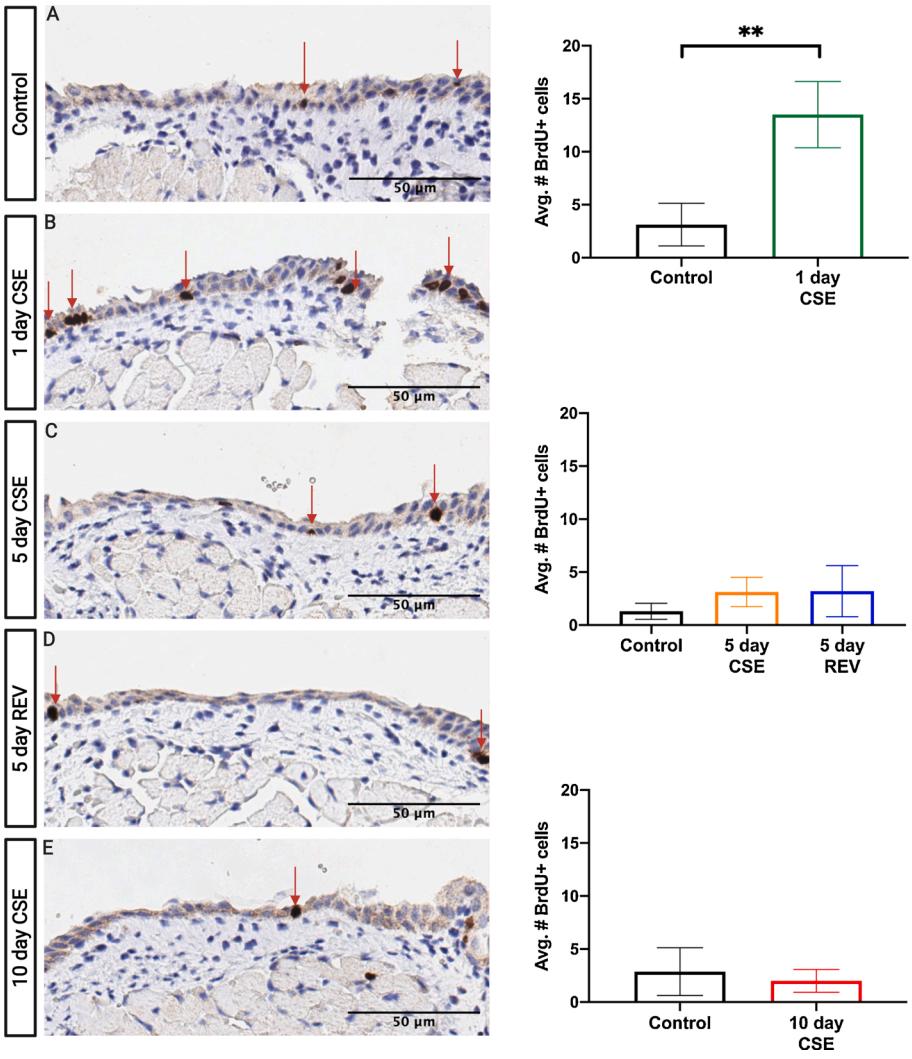

Fig. 8. VF BrdU labeled cellular proliferation. CSE significantly elevated BrdU labeled cells in VF only on day 1 (B, F). Mice in 5 day CSE (C, G) and 10 day CSE groups (E, H) had no significant changes in cellular proliferation and remained comparable to the mice in the control group (A). Reversibility evaluations in mice (D, G) had no significant increase in BrdU labeled cells. At day 1, n = 4 in control and n = 3 in CSE groups. At day 5, n = 5 in control and n = 4 in CSE groups. At day 10, n = 4 in control and n = 4 in CSE groups. n = 5 in 5 day REV group. Red single-headed arrows indicate BrdU labeled epithelial cells. Images are at a magnification of 40x. Bar graphs show the mean with SD. ** $p \leq 0.01$.

significantly increased levels of trans-3′-hydroxycotinine when compared to controls. This is not surprising as the levels of trans-3-′-hydroxycotinine are reported to be 3–4 fold higher than cotinine levels in urine [84]. Results did demonstrate significantly elevated NMR following 5 and 10 days of CSE, with NMR at day 10 being higher than on day 5. Increased NMR implies faster metabolic conversions/clearance of nicotine to cotinine and cotinine to trans-3′-hydroxycotinine [83]. Thus, increased metabolic rate leads to faster clearance of cotinine. Our finding is consistent with reports in humans that demonstrate smoking more cigarettes results in elevated NMR [83]. Evaluation of NMR in the 5 day REV group was at baseline, suggesting a decelerating rate of nicotine metabolic activity post-CS cessation. Overall, urinary biomarker analysis data is suggestive of successful CS inhalation by mice; however, is not a direct representation of CSE in the larynx. During whole body exposure, there is oral uptake of nicotine and absorption from the skin; thus, influencing levels of nicotine and its metabolites. In addition, CS administration via nose and whole body exposure can result in different pathological outcomes within the lungs [85]. Consequently, future studies should include comparison between nose only and whole body exposures in order to determine the best route of CS administration specifically to investigate laryngeal health effects of CS.

A secondary implication of an increased NMR is bodyweight reduction [86]. Nicotine in CS can cause decreased body weight via increased energy expenditure and suppression of appetite; however, these effects are reversible upon CS cessation [87]. Similarly, we observed significant body weight reduction in mice at day 5 and day 10 of CSE. Our results also indicated that there was a significant increase in body weight following CS cessation in the 5 day REV mice. The body weight post CS cessation for 5 days were comparable to control mice.

We investigated epithelial cell proliferation in the laryngeal glottic and subglottic regions following short-term CSE using the cell cycle marker BrdU. While initial increases in cell proliferation may be an adaptive response to an injurious substance, sustained cell proliferation in toxicant-exposed tissue may be a site-specific indicator of injury and identify the location and types of cells at risk for carcinogenesis [88]. We observed a significant increase in BrdU-labeled proliferative cells following only 1 day of CSE. The number of BrdU-labeled proliferative cells was comparable to controls following 5 and 10 days of exposure. This immediate response of the VF epithelium to CS may, in part, be explained by airflow dynamics. Some of the narrowest and widest regions of the upper and lower respiratory tracts are found within the larynx [9,15]. Specifically, narrowing of the glottic region creates a highly turbulent airflow, which promotes the immediate deposition of toxicants on the VF surface upon inhalation [9,89]. This may explain the early proliferative response in the glottic region on day 1. We further postulate that VF cellular proliferation attains a stable state at days 5 and 10, owing to the protective capacity of the VF epithelium. The stratified squamous epithelium of the VF is two to four cell layers thick [12]. To maintain epithelial integrity, cells undergo constant turnover where newly synthesized cells at the basement membrane differentiate and migrate through the suprabasal layers towards the luminal surfaces [12, 26]. This VF epithelium is uniquely structured such that it is designed to

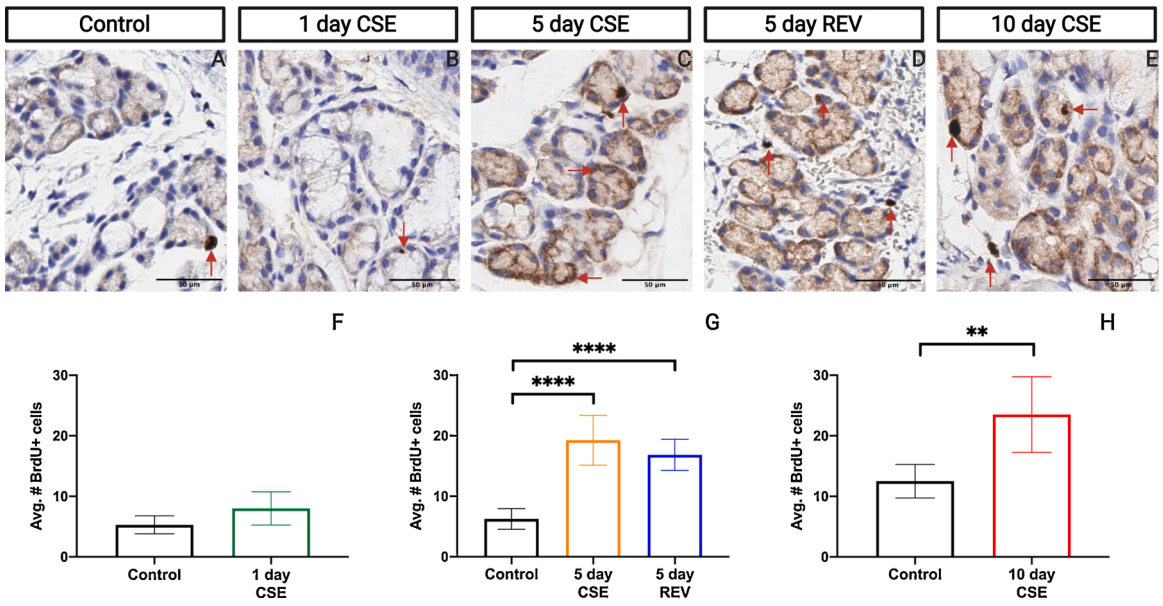

Fig. 9. Subglottic BrdU labeled cellular proliferation. CSE significantly enhanced cellular proliferation in the submucosal glands in 5 day CSE (C, G) and 10 day CSE (E, H) groups when compared to the control group (A). Mice in the 5 day REV group (D, G) had a significant increase in BrdU labeled cell populations. CSE had no impact on cellular proliferation at day 1 (B, F). At day 1, n = 5 in control and n = 4 in CSE groups. At day 5 and day 10, n = 6 in control and n = 6 in CSE groups. n = 6 in the 5 day REV group. Red single-headed arrows indicate BrdU labeled epithelial cells. Images are at a magnification of 40x. Bar graphs show the mean with SD. ** $p \leq 0.01$ and **** $p \leq 0.0001$.

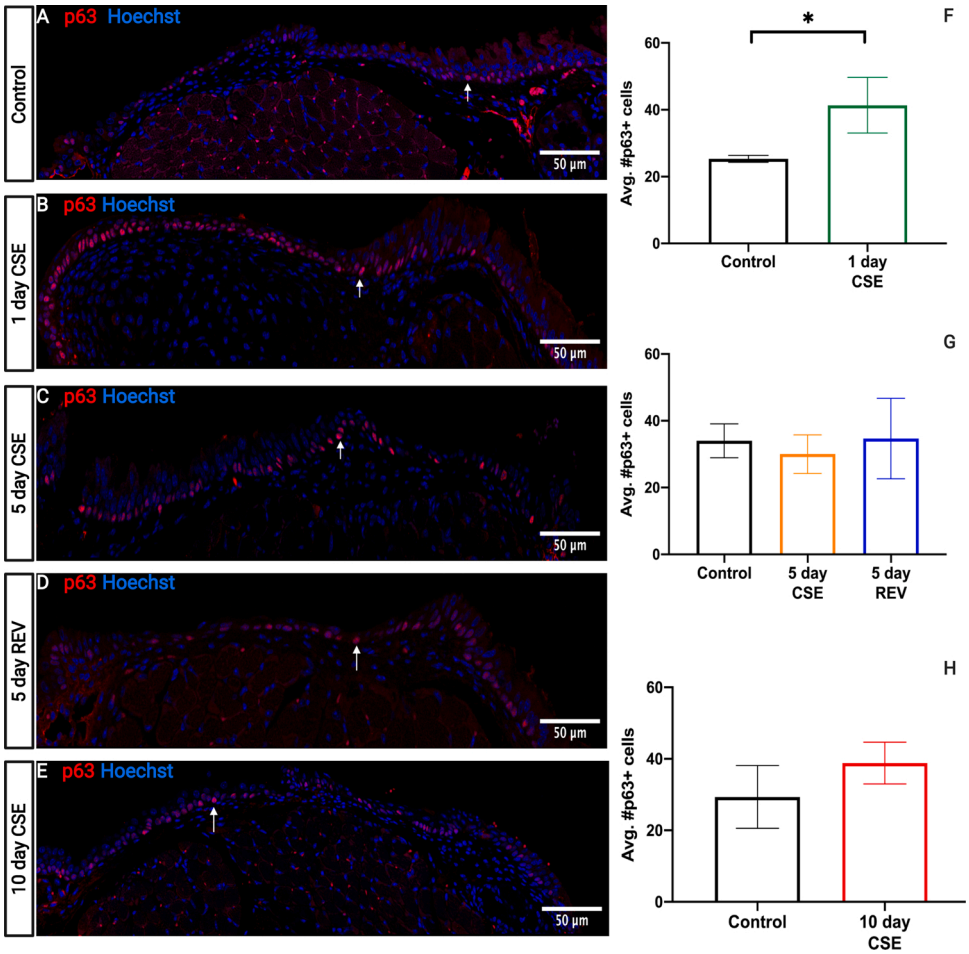

Fig. 10. VF basal cell proliferation. CSE significantly enhanced p63 labeled basal cells only on day 1 (B, F) when compared to the control group (A). Basal cell population showed no significant increase in 5 day CSE (C, G), 5 day REV (D, G), and 10 day CSE groups (E, H). n = 3 in control and CSE groups at all time points. n = 3 in 5 day REV. White single-headed arrows indicate p63 labeled basal cells. Images are at a magnification of 63x. Bar graphs show the mean with SD. * $p \leq 0.05$.

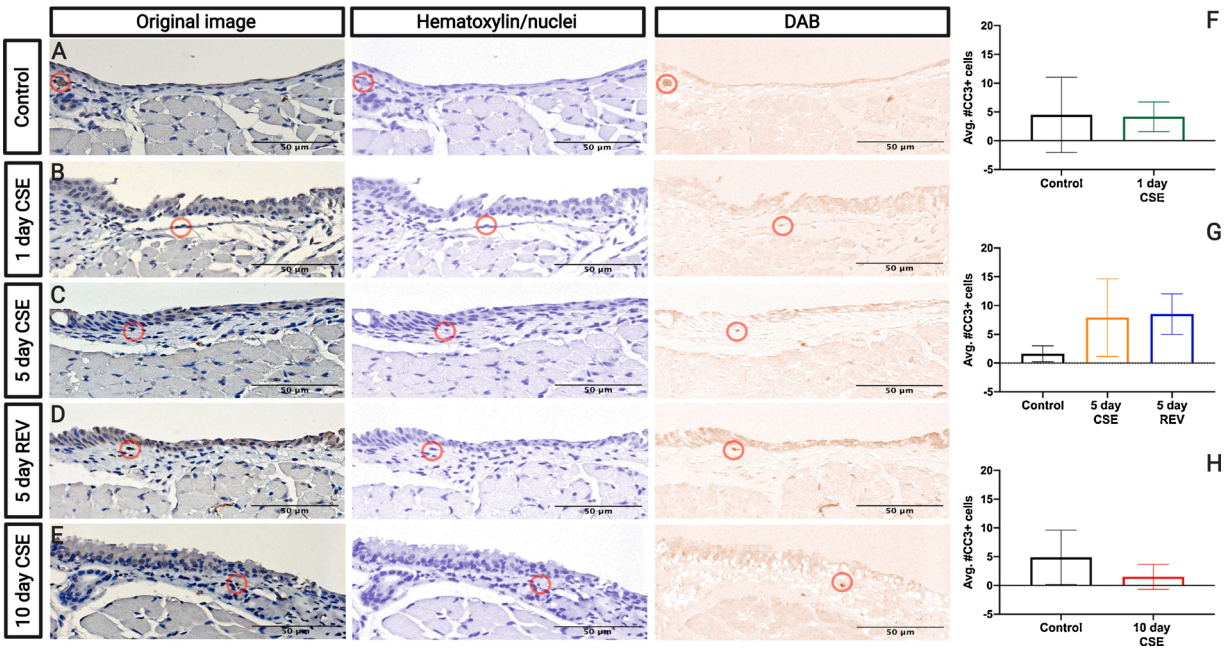

Fig. 11. Cleaved caspase-3 (CC3) apoptotic activity in VF. CSE did not alter CC3 labeled apoptotic cell populations after 1 day of CSE (B, F), 5 days of CSE (C, G), and 10 days of CSE (E, H) when compared to control (A). No alterations were seen in mice in the 5 day REV group (D, G). At day 1, n = 3 in control and CSE groups. At day 5, n = 4 in control and n = 5 in CSE groups. n = 5 in 5 day REV group. At day 10, n = 4 in control and n = 3 in the CSE group. In panel (A–E), purple channel images are hematoxylin stained nuclei and brown channel images are DAB substrates indicating CC3 positive nuclei. Red circles indicate CC3 labeled apoptotic cells. Images are at a magnification of 40x. Bar graphs show the mean with SD.

withstand repeated mechanical stresses of vibration. It has been previously reported that complete VF epithelial turnover takes approximately 96 h [12,90], which is significantly faster than other parts of the airway [26,91]. In addition, epithelial injury can further accelerate cell turnover [26]. Accelerated epithelial turnover has been previously demonstrated following iatrogenic VF injury [92–94]. We hypothesize in order to escalate epithelial cell turnover, the glottic region increased cell proliferation at day 1 as an adaptive response to CS [29], and its tolerance may be critical to maintain and protect the VF from injury, at least in the short-term. Future studies need to evaluate the factors driving the shift from a potential adaptive to a pathological response upon prolonged CSE in the glottic regions of the larynx.

In chronic CSE studies, the laryngeal epithelium exhibits hyperplasia [29,63]. In the glottic region, VF epithelial thickness, an indicator of hyperplasia, was not increased following short-term CSE. It is possible that the one-time, transient proliferative response at day 1 was so mild, that it did not induce any morphological changes and only altered the rate of turnover. Toxicological studies have reported that cell proliferation can occur without inducing morphological alterations to the epithelium in other parts of the airway like the bronchi and distal lung [95–97]. Specifically, toxicant exposures elicit initial inflammatory response, like neutrophil and macrophage influxes into the epithelium, and the migration of these cells through the epithelium can induce proliferation without epithelial changes. The unique impact of CS-induced inflammatory response on VF epithelial proliferation awaits investigation.

Given that airway basal cells function as the stem/progenitor cells of the airway epithelium, we investigated p63 positive basal cell expression in the VF following short-term CSE. In conjunction with elevated BrdU-labeled proliferative cells, we found significantly increased p63 positive basal cells on day 1, indicating basal cell hyperplasia. In the lower airways, basal cell hyperplasia is the first histologic change associated with smoking [98] and this is consistent in the VF. In addition, BrdU-labeled proliferative cells appeared confined to the p63 positive basal layer. In response to injury, such as with CSE, airway basal cells proliferate and can either regenerate normally differentiated epithelium or altered histologic phenotypes [13]. p63 expressing basal cell layers in the airway can undergo transcriptomic changes upon prolonged contact with external stimuli like CS leading to abnormal differentiation and a disorganized epithelium [99]. For example, abnormal basal cell differentiation has been associated with squamous cell metaplasia in many diseases of the respiratory tract, including the larynx [100]. Specifically, laryngeal epithelial cells exhibit squamous cell metaplasia and hyperkeratosis, in addition to epithelial hyperplasia, upon chronic exposure to CS [29,63]. Given that significant basal cell hyperplasia was only observed following 1 day of CSE, we speculate the observed pattern of a concurrent increase in p63 and BrdU immunoreactivity in VF after 1 day of CSE is likely towards promoting regeneration of normal epithelium and it is unlikely basal cells converted to squamous epithelial cells. In order to establish a timeline of events leading up to squamous conversion in the laryngeal epithelium as indicated by chronic CS studies, it will be necessary to know when and how short-term CSE initiates the conversion of basal cells to squamous differentiated cells. Consequently, future investigations should include detailed evaluation of cytokeratin expression in order to assess epithelial differentiation in the VF in response to CSE [101].

With respect to the subglottic region, our findings demonstrate that significant increases in cell proliferation in the submucosal glands begin later, on day 5, and extend to day 10 post-CSE. This region of the larynx has the highest air flow velocity, lower forces, and pressure; hence, having lesser contact with inhaled toxicants and reducing deposition [9]. Correspondingly in this study, cumulative CS inhalation for 5 and 10 days may have led to a gradual toxicant buildup in this region; consequently, triggering increased cellular proliferation. Reversibility evaluation in the subglottis showed elevated cellular proliferation post-CS cessation as well. Long-term CSE induces submucosal gland hypertrophy and mucus hypersecretion in portions of the respiratory tract including the larynx [40,41,88,102]. Although in this study, short-term CSE increased cell proliferation in the submucosal glands, submucosal gland hypertrophy was not observed. This enhanced and sustained cell proliferation may be a precursor to hypertrophy, which is likely to occur following longer CSE. Earlier reports suggest that

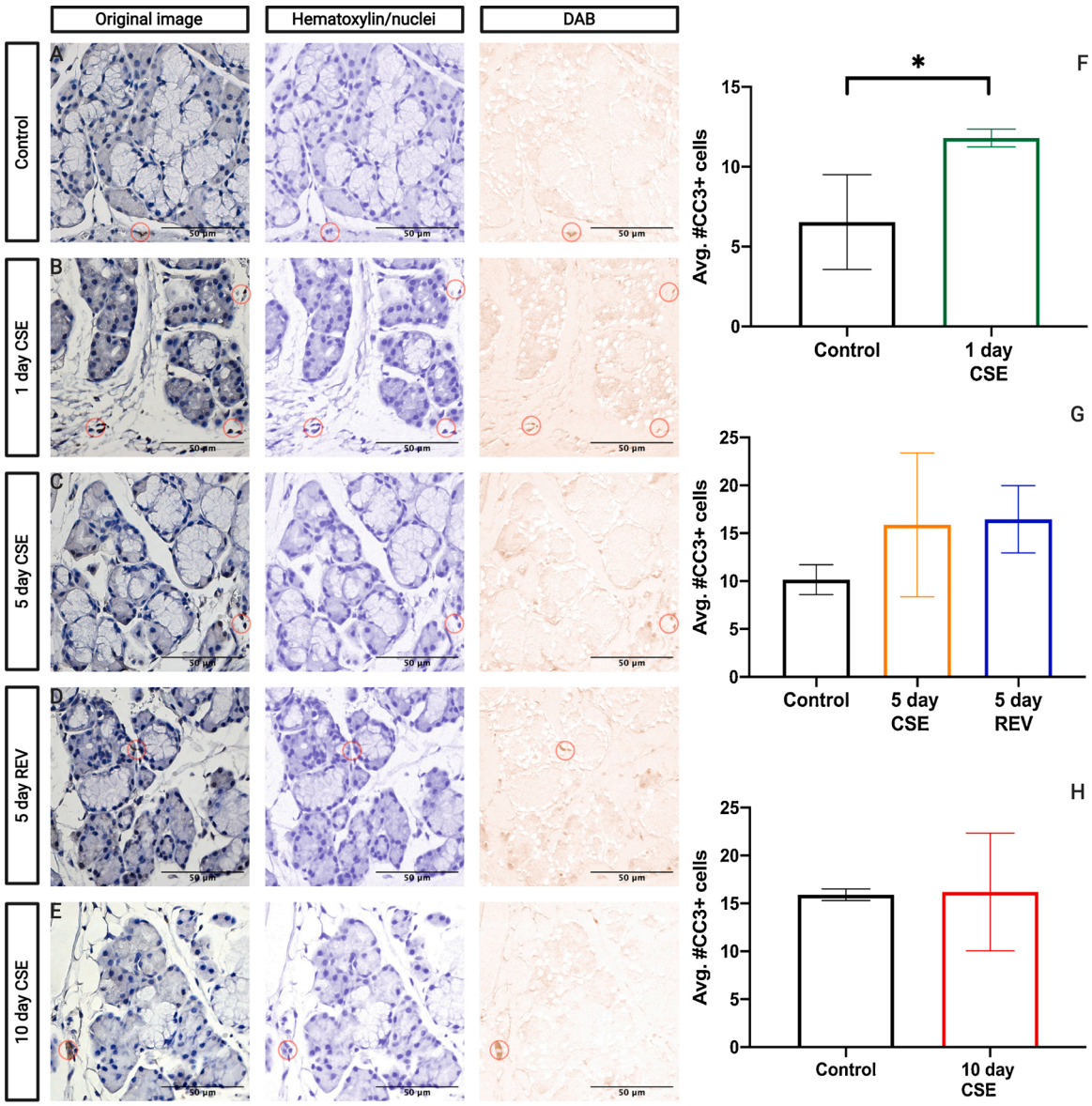

Fig. 12. Cleaved caspase-3 (CC3) apoptotic activity in subglottis. Elevated numbers of CC3 positive cells were found only at day 1 after CSE (B, F) in comparison to the controls (A). 5 day CSE (C, G), 5 day REV (D, G), and 10 day CSE (E, H) groups did not have any significant increase in CC3 levels. At day 1, n = 3 in control and CSE groups. At day 5, n = 4 in control and CSE groups. n = 4 in the 5 day REV group. At day 10, n = 3 in control and CSE groups. In panel (A–E), purple channel images are hematoxylin stained nuclei and brown channel images are DAB substrate indicating CC3 positive nuclei. Red circles indicate CC3 labeled apoptotic cells. Images are at a magnification of 40x. Bar graphs show the mean with SD. * $p \leq 0.05$.

alterations will not occur in the submucosal glands until a severe disease like condition prevails [35].

In addition to cell proliferation, cell death mechanisms are equally essential for maintaining epithelial homeostasis. During normal epithelial turnover, apoptosis is a highly regulated, inherently programmed cell death process, which expunges damaged cells without eliciting inflammatory responses [103,104]. Apoptotic signaling cascades can occur with or without being modulated by certain serine proteases called “Caspases”. Within the caspase-dependent signaling pathway, caspase 3 is a downstream enzyme that executes the final act of cellular death, upon enzyme cleaving [104,105]. Caspase independent apoptotic reactions occur via a mitochondrial pathway involving cytochrome C activity [105]. In this study, we evaluated CC3 apoptotic activity in the laryngeal mucosa and found regional differences in responses. Our results indicate increased activity in the RE-lined subglottis after 1 day of CSE. Similar findings have been demonstrated in in vitro studies in other respiratory epithelial cells present in alveoli and nasal cavities within 24 h post CSE [48,50]. In contrast, the presence of VF apoptotic activity was not detected. Reduced apoptotic levels within the VF may be due to a combination of lowered CS particle residence time and deposition fraction. Specifically, active mucociliary clearance in the larynx may have led to an overall lower CS particulate residence time in the glottic regions of the larynx. Conversely, residence time is highest in the lower respiratory tract [4,89,106]. In addition, we evaluated CS particulate deposition in the respiratory tract using the Multiple-Path Particle Dosimetry (MPPD V.3.04) [107]. Even though this model does not predict particulate deposition specific to the larynx, we utilized deposition fraction values in the tracheal region, situated immediately below the larynx, (Supplementary Fig. 2) as a comparative factor for our analysis. We conclude that CS particulate deposition is most likely less in the larynx than other regions of the lower respiratory tract (Supplementary Data S3, Supplementary Fig. 3 and Fig. 4). Several studies conducted in the human respiratory tract support this hypothesis and indicate that greater CS particulate matter is deposited in the lower

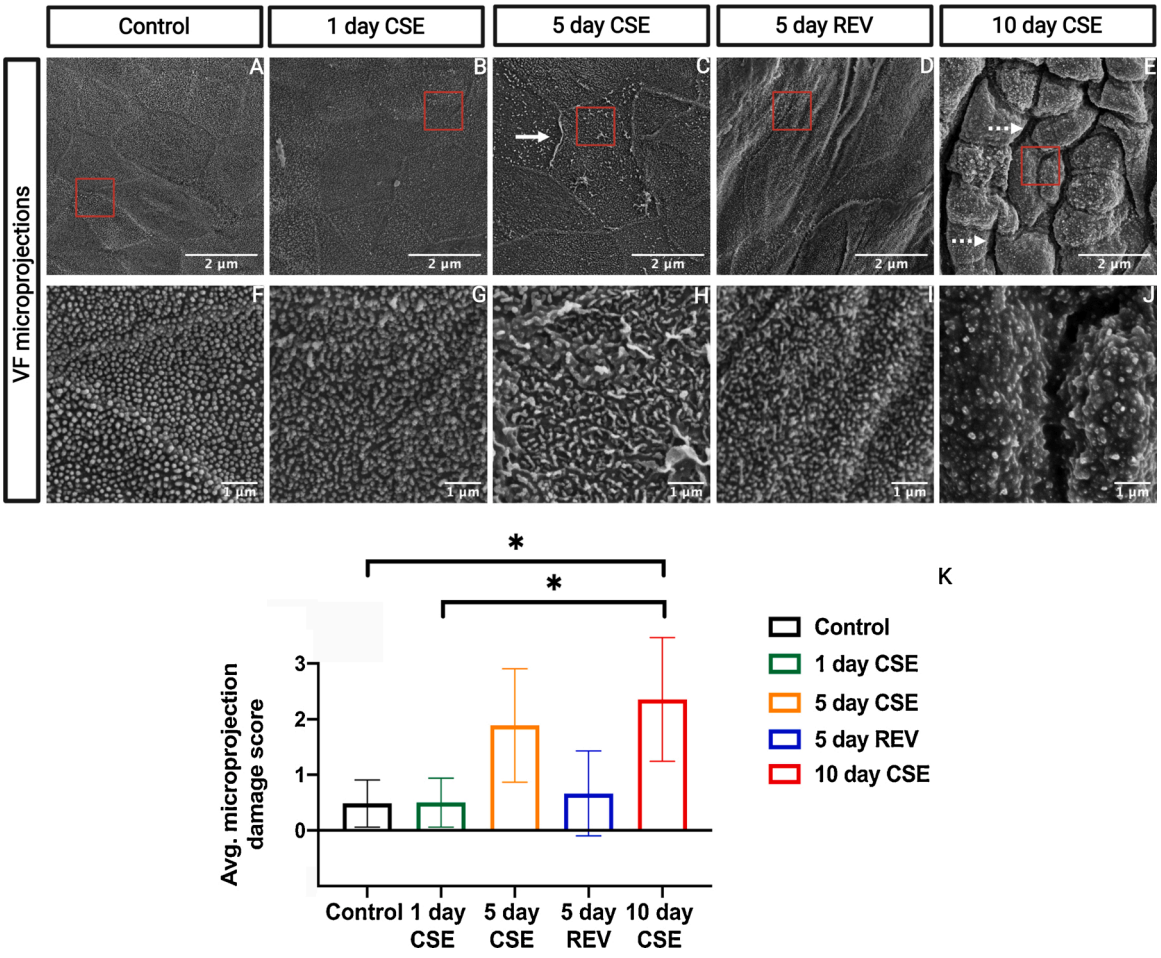

Fig. 13. SEM examination of VF epithelial surface microprojection damage and necrosis. CSE induced significant microprojection damage at day 10 (E, J, K) in comparison to the control (A, F) and 1 day CSE groups (B, G). 5 day CSE (C, H) and 5 day REV (D, I) groups did not exhibit any significant VF microprojection damage. Signs of necrosis were observed at day 5 (C) and day 10 (E) post CSE. n here indicates the number of right and left vocal folds evaluated. n = 4 in control, n = 3 in 1day CSE, 5 day CSE, 5 day REV and 10 day CSE groups. SEM images in panel (A–E), are at a magnification of 5kx and in panel (F–J), are at a magnification of 25kx. Red squares shown in 5kx images represent regions imaged at 25kx for each time point. A white single-headed arrow in the image (C) indicates necrotic epithelial sloughing/exfoliation. A white single-headed dashed arrow indicates necrotic ulceration in the image (E). Bar graphs show the mean with SD. * $p \leq 0.05$.

respiratory tract (40–57%) as compared to the upper respiratory regions (13–22%) [4,89,108].

Apoptosis can also be visually identified by SEM using certain morphological indicators like cell contraction, nuclear condensation, nuclear fragmentation, cell membrane blebbing, and by the presence of apoptotic bodies [109,110]. Our examinations of laryngeal mucosa through SEM did not reveal the presence of apoptotic cells. Cell death in response to short-term CSE may occur by other mechanisms like necrosis. Unlike apoptosis, necrosis is an accidental cell death process, where disruption of cellular plasma membranes leaks intracellular components, thereby eliciting inflammatory responses [103]. Certain features of necrosis can also be visually identified by SEM. Epithelial sloughing and ulceration have been well-associated with necrotic respiratory surfaces in response to inhaled toxicants [111,112]. Morphological evaluations of laryngeal mucosa by SEM indicated early signs of epithelial sloughing in VF after 5 days and ulcerations on the VF surface after 10 days of CSE. The occurrence of necrosis with higher doses of CS has been well documented in some in vitro studies [50,113–116]. Similarly, it is possible for necrotic processes to occur after prolonged CSE in the larynx, eliciting inflammatory responses, and contributing to disease progression. Hence, it is likely that our early SEM observations are preceding events to necrotic cell death in response to long-term CSE. In order to validate this, we will need continued efforts to evaluate CS-induced necrotic signaling mechanisms in the larynx.

Along the VF superficial epithelial cell surface, there are special substructures called microprojections [61,94]. These microprojections are believed to play a role in maintaining epithelial barrier integrity, regulating mucus secretions, and nutrient transport [61]. VF microprojections are also involved in providing traction during vocal fold vibration [117]. VF epithelial microprojections are damaged secondary to prolonged and excessive vibration [61,94]. In this study, significant microprojection damage was observed after 10 days of CSE. CSE showed an increasing trend in the extent of damage on day 5, but not significantly. It has been found that experimentally induced pathogens accumulate to a greater degree in areas of extensive damage [118]. It is possible that alterations in microprojection integrity may lead to toxicant accumulation and the pathophysiology of smoke-related VF disease. This is the first investigation to establish the impact of short-term CSE on the structure of VF epithelial microprojections. Future studies are needed to improve our understanding of the functional consequences of these changes and the role of microprojections in maintaining VF heath in response to inhaled toxicants like CS.

Cilia are specialized organelles that beat in cephalad fashion to propel inhaled toxicants trapped in the mucus layer. In the process of mucociliary clearance (MCC), mucus is transferred into the posterior larynx where it can be cleared via swallowing or expectoration [119]. Examination of the laryngeal subglottic epithelium by SEM showed signs of abnormal cilia including compound and loss of these organelles. In

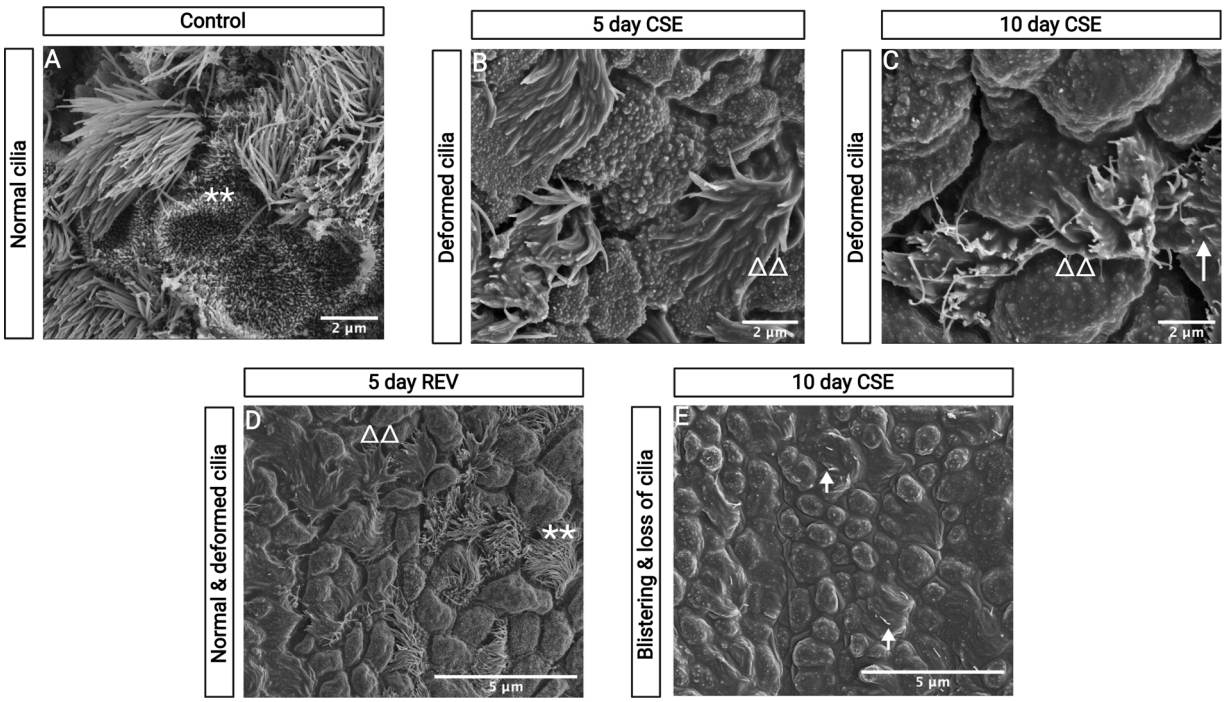

Fig. 14. SEM observations of cilia in laryngeal mucosa. In RE lined laryngeal regions, compound cilia are noticed after 5 (B) and 10 (C) days after CSE in comparison to the normal cilia in the control group (A). Reversibility evaluations (D) indicated the presence of both normal and compound cilia. Rounded cells or cellular blistering was found in RE accompanied by a ciliary loss in the 10 day CSE group (E). SEM images in panel (A–C) are at a magnification of 15kx; (D) and (E) are at a magnification of 10kx and 5kx respectively. Double triangles indicate compound cilia. Double asterisks indicate normal cilia. A white single-headed arrow indicates loss of cilia.

the lower respiratory tract, CS reduces the ciliary length, ciliary beat frequency (CBF), and causes loss of these specialized structures [120, 121], thereby impairing MCC. A proper ciliary structure is required for effective MCC; consequently, abnormal subglottic cilia likely inhibit CS toxicant clearance and promotes mucus accumulation in the larynx. Clinically, aggregation of thick, sticky mucus is observed in a smoker's larynx, leading to frequent coughing [122]. This study demonstrates the short-term CS-induced ciliary structural deformities in the larynx, potentially impacting mucus clearance impending upon prolonged CSE. It is unknown whether ciliary deformities are a result of direct damage by CS or CS-induced abnormal basal cell differentiation. Shorter cilia or ciliary loss has been attributed to abnormal basal cell differentiation in other portions of the airway [123]. This reiterates the importance of gaining a deeper understanding of the disordered basal cell differentiation characteristics in the larynx, upon short- or long-term CSE.

Although previous literature [40,41] has some limited evidence for CS-induced goblet cell hyperplasia and elevated mucin levels in the larynx, there is a paucity of information related to CS-induced mucus content changes in the laryngeal submucosal glands. We demonstrate that short- term CSE increases neutral mucus and decreases acidic mucins after 10 days of CSE. These results are consistent with short-term CSE in the rat axial airway [124]. However, other previous short- and long-term CSE studies conducted in rat trachea and axial airways, report the opposite response [88,125]. Shifts in stored mucus composition accompanied by variations in mucosal glandular size may have been implicated in disease development [126]. Correspondingly, these early shifts in mucus composition may eventually contribute to laryngeal disease development upon long-term CSE by potentially altering physical properties, MCC, and immune defense mechanisms. Subsequent studies are needed to achieve a deeper understanding of dynamic changes in neutral and acidic mucin content upon short- and long-term CSE. Furthermore, evaluation of the effect of CS on specific membrane-associated and secreted mucin glycoproteins is needed.

The current study is subject to some limitations. The larynx has a unique anatomy and we focused on the glottic and subglottic regions. Although these regions are of high clinical significance, transitional and epiglottic zones within the larynx may also be susceptible sites for CS-induced injury. Subsequent studies are needed to elucidate early cellular responses in these regions upon short-term CSE. In addition, secondary to technical issues, we were unable to collect urine samples for day 1, which limited our ability to comprehensively evaluate nicotine biomarkers and the extent of smoking associated with short-term CSE. Also, we evaluated uptake of CS particulate matter via urinary nicotine biomarker analysis only upon euthanasia. Despite our urinary nicotine biomarker analysis data supporting a successful CS inhalation by the mice, this is not representative of continuous monitoring of CS uptake. Subsequent studies also need to incorporate daily/intermittent monitoring of blood carboxyhemoglobin (COHb) in order to ensure consistent and successful CS inhalation during exposures. Furthermore, contemporary inhalation studies report measured aerosol concentration using real-time monitoring devices as well. Some studies also provide information about aerosol particle counts and physical parameters such as Geometric standard deviation (GSD) and Mass median aerodynamic diameter (MMAD), along with chemical characterization via carbon monoxide (CO) monitoring and or gravimetric filter sampling. Our future studies will incorporate such devices to monitor exposure atmosphere for precise aerosol concentration measurements, physical and chemical characterization. In terms of CS protocol, we adopted a non-intense smoking regime based on established FTC/ISO guidelines, but future studies would also benefit from incorporating Massachusetts and Canadian intense smoking standards. Also, our study demonstrated the short-term effects of the commonly used reference cigarette 3R4F, on the larynx. Although this cigarette is designed to be representative of the commonly used American blend type cigarettes, upcoming studies should include an additional CSE group by utilizing commercially available cigarettes or comparing filter vs non-filter cigarettes. In the recent years, tobacco heating products and electronic cigarettes have gained popularity as a healthier alternative to smoking conventional

cigarettes as well. Despite these newer products being less toxic than the conventional cigarettes [3,127], their ability to lessen health risks is still highly questionable. Thus, forthcoming investigations should also include toxicological evaluations of these newer alternatives in the larynx. Such comparisons will have practical implications related to human tobacco and alternative tobacco product consumption. At this juncture, we do not know which toxicants in CS are responsible for the early cellular responses seen in this study. Specific toxicants like crotonaldehyde [20] and formaldehyde [21] which are highly toxic in humans, are major CS gas/vapor phase constituents. Since laboratory rodents are obligate nasal breathers, CS inhalation can lead to significant deposition of these constituents in the upper airways capable of causing toxic effects. In fact, gas/vapor phase CS constituents can induce early morphological changes within a rat larynx [128]. Therefore, upcoming studies should aim at directly evaluating the effects of individual gas/-vapor and particulate phase CS components on the laryngeal mucosa to identify specific toxicants that drive changes. Finally, we acknowledge that the endpoints measured in the larynx in response to CS are not novel and a subset of analyses were conducted by unblinded raters. These endpoints have been validated and are well established in other parts of the respiratory tract. However, as the larynx is a relatively understudied portion of the airway, foundational studies with established endpoints are still warranted. In addition, although we primarily demonstrated good to excellent intra- and inter-rater reliability during blinded reliability analyses, the potential for bias in future studies should be reduced with use of exclusively blinded raters and / or automated analysis software.

5. Conclusions

In summary, this study is a first attempt to demonstrate the effects of short-term CSE on the laryngeal mucosa. Standard immunohistological and electron microscopy methodologies used in this study demonstrated various altered cellular responses like cell death, cell proliferation, cell surface topography changes and mucin composition in the larynx. Interaction between various factors like airflow, laryngeal anatomy, and CS characteristics including particulate deposition, give rise to regional differences in these cellular responses upon short-term CSE. This acute CS injury model helps us to identify potential adaptive mechanisms to short-term CSE as well as the location and types of cells that may be at risk for injury in the larynx following prolonged exposures. Our future studies will be focused on incorporating advanced transcriptomic methodologies like Next-Gen sequencing or spatial transcriptomics, to gain detailed insights into molecular mechanisms or pathways (innate & adaptive immune responses, oxidative stress, epithelial differentiation etc.,) involved in driving these early cellular indicators into a pathological state. Furthermore, based on the data obtained from this study, we would like to propose that future *in vivo* toxicological evaluation studies should include immunohistological (i.e., cellular proliferation, basal cell labeling) and electron microscopic techniques in their experimental design so as to visually interpret cellular responses in a toxicant exposed tissue. We believe that this will complement or strengthen accuracy of corresponding transcript level data.

Author statement

Meena Easwaran: Conceptualization, Methodology, Validation, Formal Analysis, Investigation, Resources, Writing – Original Draft, Writing – Review and Editing, Visualization

Joshua D. Martinez: Conceptualization, Formal analysis, Investigation, Resources, Writing – Review and Editing

Daniel J. Ramirez: Validation, Formal analysis, Investigation, Writing – Review and Editing

Phillip A. Gall: Validation, Formal analysis, Writing – Review and Editing

Elizabeth Erickson-DiRenzo: Conceptualization, Methodology, Validation, Formal analysis, Resources, Writing – Original Draft, Writing – Review and Editing, Visualization, Supervision, Project administration, Funding acquisition.

Funding

This study was supported by the National Institutes of Health, National Institute of Deafness and Other Communication Disorders [R21 DC016126], New Century Scholars Research Grant from the American Speech-Language-Hearing Foundation, and Mini-Seed Grant from the Stanford Nano Shared Facilities.

Declaration of Competing Interest

The authors report no declarations of interest.

Acknowledgments

We acknowledge the technical expertise provided by Dr. Nicolas Grillet (Department of Otolaryngology, Stanford University, CA, USA) for SEM sample preparation. Part of this work was performed at the Stanford Nano Shared Facilities (SNSF)/Stanford Nanofabrication Facility (SNF), supported by the National Science Foundation under award ECCS-1542152. We thank Dr. Xu Ji, and Dr. Chloe Domville-Lewis for their contributions to data collection and analysis. We also wish to thank Mr. Owen Price, Senior Scientist from Applied Research Associates Inc., Arlington, VA, USA for his technical assistance during computation CS particulate deposition using MPPD. All figures in this manuscript were created with BioRender.com.

Appendix A. Supplementary data

Supplementary material related to this article can be found, in the online version, at doi:https://doi.org/10.1016/j.toxrep.2021.04.007.

References

[1] J.T. Lariscy, Smoking-attributable mortality by cause of death in the United States: an indirect approach, SSM - Popul. Heal. 7 (2019), 100349, https://doi.org/10.1016/j.ssmph.2019.100349.
[2] S.S. Hecht, Research opportunities related to establishing standards for tobacco products under the Family Smoking Prevention and Tobacco Control Act, Nicotine Tob. Res. 14 (2011) 18–28, https://doi.org/10.1093/ntr/ntq216.
[3] D. Thorne, J. Whitwell, J. Clements, P. Walker, D. Breheny, M. Gaca, The genotoxicological assessment of a tobacco heating product relative to cigarette smoke using the in vitro micronucleus assay, Toxicol. Reports. 7 (2020) 1010–1019, https://doi.org/10.1016/j.toxrep.2020.08.013.
[4] C. Kleinstreuer, Y. Feng, Lung deposition analyses of inhaled toxic aerosols in conventional and less harmful cigarette smoke: a review, Int. J. Environ. Res. Public Health 10 (2013) 4454–4485, https://doi.org/10.3390/ijerph10094454.
[5] P. Pohunek, Development, structure and function of the upper airways, Paediatr. Respir. Rev. 5 (2004) 2–8, https://doi.org/10.1016/j.prrv.2003.09.002.
[6] C.T. Sasaki, E.M. Weaver, Physiology of the larynx, Am. J. Med. 103 (1997) 9S–18S, https://doi.org/10.1016/S0002-9343(97)00314-8.
[7] S.L. Thibeault, L. Rees, L. Pazmany, M.A. Birchall, At the crossroads: mucosal immunology of the larynx, Mucosal Immunol. 2 (2009) 122–128, https://doi.org/10.1038/mi.2008.82.
[8] J.E. Salvaggio, Inhaled particles and respiratory disease, J. Allergy Clin. Immunol. 94 (1994) 304–309, https://doi.org/10.1053/ai.1994.v94.a56009.
[9] M. Taylan, O.F. Can, M.G. Cetincakmak, M. Ozbay, Effect of airway dynamics on the development of larynx cancer, Laryngoscope. 126 (2016) 1136–1142, https://doi.org/10.1002/lary.25645.
[10] P. Schultz, Vocal fold cancer, Eur. Ann. Otorhinolaryngol. Head Neck Dis. 128 (2011) 301–308, https://doi.org/10.1016/j.anorl.2011.04.004.
[11] J.P. Dworkin-Valenti, E. Sugihara, N. Stern, I. Naumann, S. Bathula, Laryngeal Inflammation, Ann. Otolaryngol. Rhinol. 2 (2015) 1058–1065.
[12] E.E. Levendoski, C. Leydon, S.L. Thibeault, Vocal fold epithelial barrier in health and injury: a research review, J. Speech Lang. Hear. Res. 57 (2014) 1679–1691, https://doi.org/10.1044/2014_JSLHR-S-13-0283.
[13] R.G. Crystal, Airway basal cells. The “smoking gun” of chronic obstructive pulmonary disease, Am. J. Respir. Crit. Care Med. 190 (2014) 1355–1362, https://doi.org/10.1164/rccm.201408-1492PP.
[14] N.R. Hackett, R. Shaykhiev, M.S. Walters, R. Wang, R.K. Zwick, B. Ferris, B. Witover, J. Salit, R.G. Crystal, The human airway epithelial basal cell

transcriptome, PLoS One 6 (2011), https://doi.org/10.1371/journal.pone.0018378.
[15] E.E. Levendoski, M.P. Sivasankar, Vocal fold ion transport and mucin expression following acrolein exposure, J. Membr. Biol. 247 (2014) 441–450, https://doi.org/10.1007/s00232-014-9651-2.
[16] R. Talhout, T. Schulz, E. Florek, J. van Benthem, P. Wester, A. Opperhuizen, Hazardous compounds in tobacco smoke, Int. J. Environ. Res. Public Health 8 (2011) 613–628, https://doi.org/10.3390/ijerph8020613.
[17] National Research Council (US) Committee on Acute Exposure Guideline, Acrolein acute exposure guideline levels. Acute Expo. Guidel. Levels Sel. Airborne Chem, National Academies Press (US), 2010, pp. 13–48. https://www.ncbi.nlm.nih.gov/books/NBK220013/.
[18] National Research Council (US) Committee on Acute Exposure Guideline, Ammonia acute exposure guideline levels. Acute Expo. Guidel. Levels Sel. Airborne Chem, National Academies Press (US), 2008, pp. 58–114. https://www.ncbi.nlm.nih.gov/books/NBK207883/.
[19] D. Leduc, P. Gris, P. Lheureux, P.A. Gevenois, P. De Vuyst, J.C. Yernault, M. D. Leduc, Acute and long term respiratory damage following inhalation of ammonia, Thorax. 47 (1992) 755–757, https://doi.org/10.1136/thx.47.9.755.
[20] National Research Council (US) Committee on Acute Exposure Guideline, Crotonaldehyde, trans and cis + trans acute exposure guideline levels. Acute Expo. Guidel. Levels Sel. Airborne Chem, National Academies Press (US), 2008, pp. 123–172. https://www.ncbi.nlm.nih.gov/books/NBK207868/.
[21] J.A. Goris, S. Ang, C. Navarro, Laboratory safety: Minimizing the toxic effects of formaldehyde, Lab. Med. 29 (1998) 39–43, https://doi.org/10.1093/labmed/29.1.39.
[22] L.A. Buckley, X.Z. Jiang, R.A. James, K.T. Morgan, C.S. Barrow, Respiratory tract lesions induced by sensory irritants at the RD50 concentration, Toxicol. Appl. Pharmacol. 74 (1984) 417–429, https://doi.org/10.1016/0041-008X(84)90295-3.
[23] F.R. Cassee, J.P. Groten, V.J. Feron, Changes in the nasal epithelium of rats exposed by inhalation to mixtures of formaldehyde, acetaldehyde, and acrolein, Fundam. Appl. Toxicol. 29 (1996) 208–218, https://doi.org/10.1006/faat.1996.0024.
[24] W.E. Rinehart, The effect on rats of single exposures to crotonaldehyde vapor, Am. Ind. Hyg. Assoc. J. 28 (1967) 561–566, https://doi.org/10.1080/00028896709342685.
[25] E. Roemer, H.J. Anton, R. Kindt, Cell proliferation in the respiratory tract of the rat after acute inhalation of formaldehyde or acrolein, J. Appl. Toxicol. 13 (1993) 103–107, https://doi.org/10.1002/jat.2550130206.
[26] C. Leydon, R.S. Bartlett, D.A. Roenneburg, S.L. Thibeault, Localization of label-retaining cells in murine vocal fold epithelium, J. Speech Lang. Hear. Res. 54 (2011) 1060–1066, https://doi.org/10.1044/1092-4388(2010/10-0267).
[27] J. Vukelic, R. Dobrila-Dintinjana, A. Dekanic, B. Marijic, A. Cubranic, T. Braut, The relevance of assessing the cell proliferation factor ki-67 in squamous cell carcinoma of the larynx, Biomed Res. Int. 2019 (2019), https://doi.org/10.1155/2019/8142572.
[28] T.G. Osimitz, W. Droege, J.M. Finch, Toxicologic significance of histologic change in the larynx of the rat following inhalation exposure: a critical review, Toxicol. Appl. Pharmacol. 225 (2007) 229–237, https://doi.org/10.1016/j.taap.2007.08.027.
[29] R.A. Renne, K.M. Gideon, Types and patterns of response in the larynx following inhalation, Toxicol. Pathol. 34 (2006) 281–285, https://doi.org/10.1080/01926230600695631.
[30] J.M. Wojtowicz, N. Kee, BrdU assay for neurogenesis in rodents, Nat. Protoc. 1 (2006) 1399–1405, https://doi.org/10.1038/nprot.2006.224.
[31] P.R. Dodmane, L.L. Arnold, K.L. Pennington, S.M. Cohen, Orally administered nicotine induces urothelial hyperplasia in rats and mice, Toxicology. 315 (2014) 49–54, https://doi.org/10.1016/j.tox.2013.11.002.
[32] J. Li, J.C. Tharappel, S.G. Han, A.H. Cantor, E.Y. Lee, C.G. Gairola, H.P. Glauert, Effect of dietary selenium and cigarette smoke on pulmonary cell proliferation in mice, Toxicol. Sci. 111 (2009) 247–253, https://doi.org/10.1093/toxsci/kfp151.
[33] T. Ohnishi, L.L. Arnold, J. He, N.M. Clark, S. Kawasaki, S.I. Rennard, C.W. Boyer, S.M. Cohen, Inhalation of tobacco smoke induces increased proliferation of urinary bladder epithelium and endothelium in female C57BL/6 mice, Toxicology. 241 (2007) 58–65, https://doi.org/10.1016/j.tox.2007.08.088.
[34] H. Sekhon, J. Wright, A. Churg, Effects of cigarette smoke and asbestos on airway, vascular and mesothelial cell proliferation, Int. J. Exp. Pathol. 76 (1995) 411–418. https://www.ncbi.nlm.nih.gov/pmc/articles/PMC1997213/pdf/ijexpath00006-0021.pdf.
[35] J.V. Fahy, B.F. Dickey, Airway mucus function and dysfunction, N. Engl. J. Med. 363 (2010) 2233–2247, https://doi.org/10.1056/NEJMra0910061.
[36] J. Wong, B. Magun, L. Wood, Lung inflammation caused by inhaled toxicants: a review, Int. J. Chron. Obstruct. Pulmon. Dis. 11 (2016) 1391, https://doi.org/10.2147/COPD.S106009.
[37] X. Cao, Y. Wang, R. Xiong, L. Muskhelishvili, K. Davis, P.A. Richter, R.H. Heflich, Cigarette whole smoke solutions disturb mucin homeostasis in a human in vitro airway tissue model, Toxicology. 409 (2018) 119–128, https://doi.org/10.1016/j.tox.2018.07.015.
[38] T. Hadar, E. Yaniv, Y. Shvili, R. Koren, J. Shvero, Histopathological changes of the nasal mucosa induced by smoking, Inhal. Toxicol. 21 (2009) 1119–1122, https://doi.org/10.3109/08958370902767070.
[39] Y.A. Mebratu, K. Schwalm, K.R. Smith, M. Schuyler, Y. Tesfaigzi, Cigarette smoke suppresses bik to cause epithelial cell Hyperplasia and mucous cell metaplasia, Am. J. Respir. Crit. Care Med. 183 (2011) 1531–1538, https://doi.org/10.1164/rccm.201011-1930OC.
[40] D.A. Mouadeb, P.C. Belafsky, M. Birchall, C. Hood, T. Konia, K.E. Pinkerton, The effects of allergens and tobacco smoke on the laryngeal mucosa of guinea pigs, Otolaryngol. Neck Surg. 140 (2009) 493–497, https://doi.org/10.1016/j.otohns.2008.12.034.
[41] R. Ueha, S. Ueha, K. Kondo, T. Nito, Y. Fujimaki, H. Nishijima, K. Tsunoda, F.H. W. Shand, K. Matsushima, T. Yamasoba, Laryngeal mucus hypersecretion is exacerbated after smoking cessation and ameliorated by glucocorticoid administration, Toxicol. Lett. 265 (2017) 140–146, https://doi.org/10.1016/j.toxlet.2016.11.023.
[42] R.D. Nikumbh, D.B. Nikumbh, B.N. Umarji, Mucin histochemical study of the colon in normal and malignant lesions, Int. J. Health Sci. Res. 2 (2012) 20–32.
[43] K.O. Danquah, E. Adjei, S. Quayson, E. Adankwah, D. Gyamfi, P.P.S. Ossei, G. Dzikunu, P. Mensah, C. Lepkor, Mucin expression patterns in histological grades of colonic cancers in Ghanaian population, Pan Afr. Med. J. 27 (2017), https://doi.org/10.11604/pamj.2017.27.267.9793.
[44] R.J. Chen, L.W. Chang, P. Lin, Y.-J. Wang, Epigenetic effects and molecular mechanisms of tumorigenesis induced by cigarette smoke: an overview, J. Oncol. 2011 (2011), 654931, https://doi.org/10.1155/2011/654931.
[45] S.P. Faux, T. Tai, D. Thorne, Y. Xu, D. Breheny, M. Gaca, The role of oxidative stress in the biological responses of lung epithelial cells to cigarette smoke, Biomarkers. 14 (2009) 90–96, https://doi.org/10.1080/13547500902965047.
[46] V.J. Feron, J.H.E. Arts, C.F. Kuper, P.J. Slootweg, R.A. Woutersen, Health risks associated with inhaled nasal toxicants, Crit. Rev. Toxicol. 31 (2001) 313–347, https://doi.org/10.1080/20014091111712.
[47] A. Aoshiba K, Nagai, Oxidative stress, cell death, and other damage to alveolar epithelial cells induced by cigarette smoke, Tob. Induc. Dis. 1 (2003), https://doi.org/10.1186/1617-9625-1-3-219.
[48] D.M. Comer, J.S. Elborn, M. Ennis, Inflammatory and cytotoxic effects of acrolein, nicotine, acetylaldehyde and cigarette smoke extract on human nasal epithelial cells, BMC Pulm. Med. 14 (2014), https://doi.org/10.1186/1471-2466-14-32.
[49] A. Kode, S.R. Yang, I. Rahman, Differential effects of cigarette smoke on oxidative stress and proinflammatory cytokine release in primary human airway epithelial cells and in a variety of transformed alveolar epithelial cells, Respir. Res. 7 (2006), https://doi.org/10.1186/1465-9921-7-132.
[50] B. Kosmider, E.M. Messier, H.W. Chu, R.J. Mason, Human alveolar epithelial cell injury induced by cigarette smoke, PLoS One 6 (2011), https://doi.org/10.1371/journal.pone.0026059.
[51] S. Suzuki, S.M. Cohen, L.L. Arnold, H. Kato, S. Fuji, K.L. Pennington, Y. Nagayasu, A. Naiki-Ito, Y. Yamashita, S. Takahashi, Orally administered nicotine effects on rat urinary bladder proliferation and carcinogenesis, Toxicology. 398–399 (2018) 31–40, https://doi.org/10.1016/j.tox.2018.02.008.
[52] S. Verschuere, K.R. Bracke, T. Demoor, M. Plantinga, P. Verbrugghe, L. Ferdinande, B.N. Lambrecht, G.G.G. Brusselle, C.A. Cuvelier, Cigarette smoking alters epithelial apoptosis and immune composition in murine GALT, Lab. Investig. 91 (2011) 1056–1067, https://doi.org/10.1038/labinvest.2011.74.
[53] S. Ito, K. Ishimori, S. Ishikawa, Effects of repeated cigarette smoke extract exposure over one month on human bronchial epithelial organotypic culture, Toxicol. Reports. 5 (2018) 864–870, https://doi.org/10.1016/j.toxrep.2018.08.015.
[54] Y.S. Ding, P. Richter, B. Hearn, L. Zhang, R. Bravo, X. Yan, J.J. Perez, M. Chan, J. Hughes, P. Chen, W. Chen, J. Wong, S. Holmberg, S. Smith, M. Larango, L. Valentín-Blasini, C.H. Watson, Chemical characterization of mainstream smoke from SPECTRUM variable nicotine research cigarettes, Tob. Regul. Sci. 3 (2017) 81–94, https://doi.org/10.18001/trs.3.1.8.
[55] S.M. Reilly, R. Goel, Z. Bitzer, R.J. Elias, J. Foulds, J. Muscat, J.P. Richie, Effects of topography-related puff parameters on carbonyl delivery in mainstream cigarette smoke, Chem. Res. Toxicol. 30 (2017) 1463–1469, https://doi.org/10.1021/acs.chemrestox.7b00104.
[56] R. Goel, Z.T. Bitzer, S.M. Reilly, J. Foulds, J. Muscat, R.J. Elias, J.P. Richie, Influence of smoking puff parameters and tobacco varieties on free radicals yields in cigarette mainstream smoke, Chem. Res. Toxicol. 31 (2018) 325–331, https://doi.org/10.1021/acs.chemrestox.8b00011.
[57] G. Jaccard, D.T. Djoko, A. Korneliou, R. Stabbert, M. Belushkin, M. Esposito, Mainstream smoke constituents and in vitro toxicity comparative analysis of 3R4F and 1R6F reference cigarettes, Toxicol. Reports. 6 (2019) 222–231, https://doi.org/10.1016/j.toxrep.2019.02.009.
[58] V. Lungova, J.M. Verheyden, J. Herriges, X. Sun, S.L. Thibeault, Ontogeny of the mouse vocal fold epithelium, Dev Biol. Dev Biol. 399 (2) (2015) 263–282, https://doi.org/10.1016/j.ydbio.2014.12.037.
[59] C.R. Watts, J.A. Marler, B. Rousseau, Qualitative characterization of elastic Fiber distribution in the mouse vocal fold: further development of an animal model, J. Voice 25 (2011) e1–e6, https://doi.org/10.1016/j.jvoice.2009.07.010.
[60] C.G. Jones, Scanning electron microscopy: preparation and imaging for SEM, in: L.S. Bell (Ed.), Forensic Microsc. Skelet. Tissues Methods Protoc., Humana Press, Totowa, NJ, 2012, pp. 1–20, https://doi.org/10.1007/978-1-61779-977-8_1.
[61] T. Kojima, M. Van Deusen, W.G. Jerome, C.G. Garrett, M.P. Sivasankar, C. K. Novaleski, B. Rousseau, Quantification of acute vocal fold epithelial surface damage with increasing time and magnitude doses of vibration exposure, PLoS One 9 (2014), https://doi.org/10.1371/journal.pone.0091615.
[62] G. Perinetti, A series of basic statistics articles for clinical research: StaTips view project radiographical indicators of mandibular growth spurt view project, Artic. South Eur. J. Orthod. Dentofac. Res. (2018), https://doi.org/10.5937/sejodr5-17434.
[63] D.J. Lewis, Factors affecting the distribution of tobacco smoke-induced lesions in the rodent larynx, Toxicol. Lett. 9 (1981) 189–194, https://doi.org/10.1016/0378-4274(81)90039-4.

[64] X. Liu, A. Mustonen, W. Zheng, M.P. Sivasankar, A.C. Durkes, Cigarette smoke exposure to pig larynx in an inhalation chamber, J. Voice 33 (2019) 846–850, https://doi.org/10.1016/j.jvoice.2018.05.005.
[65] L.B. Thomas, J.C. Stemple, R.D. Andreatta, F.H. Andrade, Establishing a new animal model for the study of laryngeal biology and disease: an anatomic study of the mouse larynx, J. Speech Lang. Hear. Res. 52 (2009) 802–811, https://doi.org/10.1044/1092-4388(2008/08-0087).
[66] C.R.E. Coggins, A review of chronic inhalation studies with mainstream cigarett smoke in rats and mice, Toxicol. Pathol. 26 (1998) 307–314, https://doi.org/10.1177/019262339802600301.
[67] C.R.E. Coggins, An updated review of inhalation studies with cigarette smoke in laboratory animals, Int. J. Toxicol. 26 (2007) 331–338, https://doi.org/10.1080/10915810701490190.
[68] E. Erickson-DiRenzo, S.P. Singh, J.D. Martinez, S.E. Sanchez, M. Easwaran, T. A. Valdez, Cigarette smoke-induced changes in the murine vocal folds: a Raman spectroscopic observation, Analyst. 145 (2020) 7709–7717, https://doi.org/10.1039/d0an01570a.
[69] OECD, Test No. 412: Subacute Inhalation Toxicity: 28-Day Study, OECD, 2018, https://doi.org/10.1787/9789264070783-en.
[70] Organisation for Economic Co-operation and Development, Test No. 413: Subchronic Inhalation Toxicity: 90-day Study, OECD Publishing, 2018, https://doi.org/10.1787/9789264070806-en.
[71] J.J. Piadé, E. Roemer, R. Dempsey, H. Weiler, K. Meurrens, P. Vanscheeuwijck, M. K. Schorp, Toxicological assessment of kretek cigarettes part 3: kretek and American-blended cigarettes, inhalation toxicity, Regul. Toxicol. Pharmacol. 70 (2014) S26–S40, https://doi.org/10.1016/j.yrtph.2014.09.013.
[72] U. Kogel, W.K. Schlage, F. Martin, Y. Xiang, S. Ansari, P. Leroy, P. Vanscheeuwijck, S. Gebel, A. Buettner, C. Wyss, M. Esposito, J. Hoeng, M. C. Peitsch, A 28-day rat inhalation study with an integrated molecular toxicology endpoint demonstrates reduced exposure effects for a prototypic modified risk tobacco product compared with conventional cigarettes, Food Chem. Toxicol. 68 (2014) 204–217, https://doi.org/10.1016/j.fct.2014.02.034.
[73] H. Fujimoto, H. Tsuji, C. Okubo, I. Fukuda, T. Nishino, K.M. Lee, R. Renne, H. Yoshimura, Biological responses in rats exposed to mainstream smoke from a heated cigarette compared to a conventional reference cigarette, Inhal. Toxicol. 27 (2015) 224–236, https://doi.org/10.3109/08958378.2015.1027799.
[74] B.A. Wong, P.W. Ross, R.A. James, Development and use of a single-animal whole-body system for inhalation exposure, Lab. Anim. 37 (2008) 33–40, https://doi.org/10.1038/laban0108-33.
[75] H. Tsuji, K.M. Lee, K. Yoshino, H. Nakamura, G. Lulham, R. Renne, H. Yoshimura, Comparison of the physiological and morphological effects of cigarette smoke exposure at comparable weekly doses on Sprague-Dawley rats, Inhal. Toxicol. 23 (2011) 17–32, https://doi.org/10.3109/08958378.2010.537396.
[76] H. Tsuji, H. Fujimoto, D. Matsuura, T. Nishino, M. Lee, H. Yoshimura, Comparison of biological responses in rats under various cigarette smoke exposure conditions, J. Toxicol. Pathol. 26 (2013) 159–174, https://doi.org/10.1293/tox.26.159.
[77] A. Dalrymple, P. Ordoñez, D. Thorne, D. Walker, O.M. Camacho, A. Büttner, D. Dillon, C. Meredith, Cigarette smoke induced genotoxicity and respiratory tract pathology: evidence to support reduced exposure time and animal numbers in tobacco product testing, Inhal. Toxicol. 28 (2016) 324–338, https://doi.org/10.3109/08958378.2016.1170911.
[78] D.W. Gaylor, The use of Haber's law in standard setting and risk assessment, Toxicology. 149 (2000) 17–19, https://doi.org/10.1016/S0300-483X(00)00228-6.
[79] F.J. Miller, P.M. Schlosser, D.B. Janszen, Haber's rule: a special case in a family of curves relating concentration and duration of exposure to a fixed level of response for a given endpoint, Toxicology. 149 (2000) 21–34, https://doi.org/10.1016/S0300-483X(00)00229-8.
[80] D. Shusterman, E. Matovinovic, A. Salmon, Does Haber's law apply to human sensory irritation? Inhal. Toxicol. 18 (2006) 457–471, https://doi.org/10.1080/08958370600602322.
[81] T.H. Thatcher, R.P. Benson, R.P. Phipps, P.J. Sime, High-dose but not low-dose mainstream cigarette smoke suppresses allergic airway inflammation by inhibiting T cell function, Am. J. Physiol. - Lung Cell. Mol. Physiol. 295 (2008) L412, https://doi.org/10.1152/ajplung.00392.2007.
[82] E.L. Carmines, C.L. Gaworski, A.S. Faqi, N. Rajendran, In utero exposure to 1R4F reference cigarette smoke: evaluation of developmental toxicity, Toxicol. Sci. 75 (2003) 134–147, https://doi.org/10.1093/toxsci/kfg155.
[83] N.L. Benowitz, O.F. Pomerleau, C.S. Pomerleau, P. Jacob, Nicotine metabolite ratio as a predictor of cigarette consumption, Nicotine Tob. Res. 5 (2003) 621–624, https://doi.org/10.1080/1462220031000158717.
[84] P. Jacob, L. Yu, M. Duan, L. Ramos, O. Yturralde, N.L. Benowitz, Determination of the nicotine metabolites cotinine and trans-3'-hydroxycotinine in biologic fluids of smokers and non-smokers using liquid chromatography-tandem mass spectrometry: biomarkers for tobacco smoke exposure and for phenotyping cytochrome P450 2A6 activity, J. Chromatogr. B Anal. Technol. Biomed. Life Sci. 879 (2011) 267–276, https://doi.org/10.1016/j.jchromb.2010.12.012.
[85] G.M. Curtin, M.A. Higuchi, P.H. Ayres, J.E. Swauger, A.T. Mosberg, Lung tumorigenicity in A/J and rasH2 transgenic mice following mainstream tobacco smoke inhalation, Toxicol. Sci. 81 (2004) 26–34, https://doi.org/10.1093/toxsci/kfh175.
[86] A.E. Taylor, R.C. Richmond, T. Palviainen, A. Loukola, R.E. Wootton, J. Kaprio, C. L. Relton, G.D. Smith, M.R. Munafò, The effect of body mass index on smoking behaviour and nicotine metabolism: a Mendelian randomization study, Hum. Mol. Genet. 28 (2019) 1322–1330, https://doi.org/10.1093/hmg/ddy434.
[87] J. Audrain-Mcgovern, N.L. Benowitz, Cigarette smoking, nicotine, and body weight, Clin. Pharmacol. Ther. 90 (2011) 164–168, https://doi.org/10.1038/clpt.2011.105.
[88] T.H. March, L.M. Kolar, E.B. Barr, G.L. Finch, M.G. Ménache, K.J. Nikula, Enhanced pulmonary epithelial replication and axial airway mucosubstance changes in F344 rats exposed short-term to mainstream cigarette smoke, Toxicol. Appl. Pharmacol. 161 (1999) 171–179, https://doi.org/10.1006/taap.1999.8798.
[89] Z. Zhang, C. Kleinstreuer, S. Hyun, Size-change and deposition of conventional and composite cigarette smoke particles during inhalation in a subject-specific airway model, J. Aerosol Sci. 46 (2012) 34–52, https://doi.org/10.1016/j.jaerosci.2011.12.002.
[90] V. Savelli, R. Rizzoli, E. Rizzi, A. Galanzi, A. Buffa, R. Rana, G. Lattanzi, B. Baratta, Cell kinetics of vocal fold epithelium in rats, Boll. Della Soc. Ital. Di Biol. Sper. 67 (1991) 1081–1088.
[91] E.L. Rawlins, B.L.M. Hogan, Ciliated epithelial cell lifespan in the mouse trachea and lung, Am. J. Physiol. - Lung Cell. Mol. Physiol. 295 (2008), https://doi.org/10.1152/ajplung.90209.2008.
[92] R.C. Branski, K. Verdolini, C.A. Rosen, P.A. Hebda, Acute vocal fold wound healing in a rabbit model, Ann. Otol. Rhinol. Laryngol. 114 (2005) 19–24, https://doi.org/10.1177/000348940511400105.
[93] C. Leydon, M. Imaizumi, R.S. Bartlett, S.F. Wang, S.L. Thibeault, Epithelial cells are active participants in vocal fold wound healing: an in vivo animal model of injury, PLoS One 9 (2014), e115389, https://doi.org/10.1371/journal.pone.0115389.
[94] B. Rousseau, T. Kojima, C.K. Novaleski, E.E. Kimball, C.V. Valenzuela, M. Mizuta, J.J. Daniero, C. Gaelyn Garrett, M. Preeti Sivasankar, Recovery of vocal fold epithelium after acute phonotrauma, Cells Tissues Organs (Print) 204 (2017) 93–104, https://doi.org/10.1159/000472251.
[95] N.A. Hackett, Cell proliferation in lung following acute fly ash exposure, Toxicology. 27 (1983) 273–286, https://doi.org/10.1016/0300-483X(83)90023-9.
[96] K.P. Keenan, U. Saffiotti, S.F. Stinson, C.W. Riggs, E.M. McDowell, Morphological and cytokinetic responses of Hamster airways to intralaryngeal or intratracheal cannulation with instillation of saline or ferric oxide particles in saline, Cancer Res. 49 (6) (1989) 1521–1527.
[97] S.G. Shami, M.J. Evans, L.A. Martinez, Type II cell proliferation related to migration of inflammatory cells into the lung, Exp. Mol. Pathol. 44 (1986) 344–352, https://doi.org/10.1016/0014-4800(86)90048-1.
[98] D.M. Ryan, T.L. Vincent, J. Salit, M.S. Walters, F. Agosto-Perez, Smoking dysregulates the human airway basal cell transcriptome at COPD risk locus 19q13.2, PLoS One 9 (2014), 88051, https://doi.org/10.1371/journal.pone.0088051.
[99] G.D. Amatngalim, W. Broekman, N.M. Daniel, L.E.P.M. Van Der Vlugt, A. Van Schadewijk, C. Taube, P.S. Hiemstra, Cigarette smoke modulates repair and innate immunity following injury to airway epithelial cells, PLoS One 11 (2016), https://doi.org/10.1371/journal.pone.0166255.
[100] J.R. Rock, S.H. Randell, B.L.M. Hogan, Airway basal stem cells: a perspective on their roles in epithelial homeostasis and remodeling, DMM Dis, Model. Mech. 3 (2010) 545–556, https://doi.org/10.1242/dmm.006031.
[101] W.K. Schlage, H. Bulles, D. Friedrichs, M. Kuhn, A. Teredesai, Cytokeratin expression patterns in the rat respiratory tract as markers of epithelial differentiation in inhalation toxicology. I. Determination of normal cytokeratin expression patterns in nose, larynx, trachea, and lung, Toxicol. Pathol. 26 (1998) 324–343, https://doi.org/10.1177/019262339802600307.
[102] J.A. Hotchkiss, W.A. Evans, B.T. Chen, G.L. Finch, J.R. Harkema, Regional differences in the effects of mainstream cigarette smoke on stored mucosubstances and DNA synthesis in F344 rat nasal respiratory epithelium, Toxicol. Appl. Pharmacol. 131 (1995) 316–324, https://doi.org/10.1006/taap.1995.1074.
[103] B. Messner, S. Frotschnig, A. Steinacher-Nigisch, B. Winter, E. Eichmair, J. Gebetsberger, S. Schwaiger, C. Ploner, G. Laufer, D. Bernhard, Apoptosis and necrosis: two different outcomes of cigarette smoke condensate-induced endothelial cell death, Cell Death Dis. 3 (2012) e424, https://doi.org/10.1038/cddis.2012.162.
[104] S.R. White, Apoptosis and the airway epithelium, J. Allergy (Cairo) 2011 (2011), 948406, https://doi.org/10.1155/2011/948406.
[105] L.E. Bröker, F.A.E. Kruyt, G. Giaccone, Cell death independent of caspases: a review, Clin. Cancer Res. 11 (2005) 3155, https://doi.org/10.1158/1078-0432.CCR-04-2223.
[106] S.K. Sahu, M. Tiwari, R.C. Bhangare, G.G. Pandit, Particle size distribution of mainstream and exhaled cigarette smoke and predictive deposition in human respiratory tract, Aerosol Air Qual. Res. 13 (2013) 324–332, https://doi.org/10.4209/aaqr.2012.02.0041.
[107] B. Asgharian, O.T. Price, M. Oldham, L.C. Chen, E.L. Saunders, T. Gordon, V. B. Mikheev, K.R. Minard, J.G. Teeguarden, Computational modeling of nanoscale and microscale particle deposition, retention and dosimetry in the mouse respiratory tract, Inhal. Toxicol. 26 (2014) 829–842, https://doi.org/10.3109/08958378.2014.935535.
[108] R.R. Baker, M. Dixon, The retention of tobacco smoke constituents in the human respiratory tract, Inhal. Toxicol. 18 (2006) 255–294, https://doi.org/10.1080/08958370500444163.
[109] S. Burattini, E. Falcieri, Analysis of cell death by electron microscopy, in: K. McCall, C. Klein (Eds.), Necrosis Methods Protoc., Humana Press, Totowa, NJ, 2013, pp. 77–89, https://doi.org/10.1007/978-1-62703-383-1_7.

[110] G.R. Wickman, L. Julian, K. Mardilovich, S. Schumacher, J. Munro, N. Rath, S. Al Zander, A. Mleczak, D. Sumpton, N. Morrice, W.V. Bienvenut, M.F. Olson, Blebs produced by actin-myosin contraction during apoptosis release damage-associated molecular pattern proteins before secondary necrosis occurs, Cell Death Differ. 20 (2013) 1293–1305, https://doi.org/10.1038/cdd.2013.69.

[111] R.A. Renne, K.M. Gideon, S.J. Harbo, L.M. Staska, S.L. Grumbein, Upper respiratory tract lesions in inhalation toxicology, Toxicol. Pathol. 35 (2007) 163–169, https://doi.org/10.1080/01926230601052667.

[112] R. Renne, A. Brix, J. Harkema, R. Herbert, B. Kittel, D. Lewis, T. March, K. Nagano, M. Pino, S. Rittinghausen, M. Rosenbruch, P. Tellier, T. Wohrmann, Proliferative and nonproliferative lesions of the rat and mouse respiratory tract, Toxicol. Pathol. 37 (2009) 5S–73S, https://doi.org/10.1177/0192623309353423.

[113] Y. Hoshino, T. Mio, S. Nagai, H. Miki, I. Ito, T. Izumi, Cytotoxic effects of cigarette smoke extract on an alveolar type II cell-derived cell line, Am. J. Physiol. Cell. Mol. Physiol. 281 (2001) L509–L516, https://doi.org/10.1152/ajplung.2001.281.2.L509.

[114] T. Ishii, T. Matsuse, H. Igarashi, M. Masuda, S. Teramoto, Y. Ouchi, Tobacco smoke reduces viability in human lung fibroblasts: protective effect of glutathioneS-transferase P1, Am. J. Physiol. Cell. Mol. Physiol. 280 (2001) L1189–L1195, https://doi.org/10.1152/ajplung.2001.280.6.L1189.

[115] D.J. Slebos, S.W. Ryter, M. van der Toorn, F. Liu, F. Guo, C.J. Baty, J.M. Karlsson, S.C. Watkins, H.P. Kim, X. Wang, J.S. Lee, D.S. Postma, H.F. Kauffman, A.M. K. Choi, Mitochondrial localization and function of heme Oxygenase-1 in cigarette smoke–Induced cell death, Am. J. Respir. Cell Mol. Biol. 36 (2007) 409–417, https://doi.org/10.1165/rcmb.2006-0214OC.

[116] M. Vayssier, N. Banzet, D. François, K. Bellmann, B.S. Polla, Tobacco smoke induces both apoptosis and necrosis in mammalian cells: differential effects of HSP70, Am. J. Physiol. Cell. Mol. Physiol. 275 (1998) L771–L779, https://doi.org/10.1152/ajplung.1998.275.4.L771.

[117] S.D. Gray, Cellular physiology of the vocal folds, Otolaryngol. Clin. North Am. 33 (2000) 679–697, https://doi.org/10.1016/S0030-6665(05)70237-1.

[118] J.L. Sokol, S.K. Masur, P.A. Asbell, J.M. Wolosin, Layer-by-layer desquamation of corneal epithelium and maturation of tear-facing membranes, Invest. Ophthalmol. Vis. Sci. 31 (1990) 294–304.

[119] X.M. Bustamante-Marin, L.E. Ostrowski, Cilia and mucociliary clearance, cold spring harb, Perspect. Biol. Med. 9 (2017), https://doi.org/10.1101/cshperspect.a028241.

[120] P.L. Leopold, M.J. O'Mahony, X. Julie Lian, A.E. Tilley, B.G. Harvey, R.G. Crystal, Smoking is associated with shortened airway cilia, PLoS One 4 (2009), https://doi.org/10.1371/journal.pone.0008157.

[121] S.M. Simet, J.H. Sisson, J.A. Pavlik, J.M. DeVasure, C. Boyer, X. Liu, S. Kawasaki, J.G. Sharp, S.I. Rennard, T.A. Wyatt, Long-term cigarette smoke exposure in a mouse model of ciliated epithelial cell function, Am. J. Respir. Cell Mol. Biol. 43 (2010) 635–640, https://doi.org/10.1165/rcmb.2009-0297OC.

[122] M. Richardson, The physiology of mucus and sputum production in the respiratory system, Nurs. Times 99 (23) (2003) 63–64.

[123] R.S. Deeb, M.S. Walters, Y. Strulovici-Barel, Q. Chen, S.S. Gross, R.G. Crystal, Smoking-associated disordering of the airway basal stem/progenitor cell metabotype, Am. J. Respir. Cell Mol. Biol. 54 (2016) 231–240, https://doi.org/10.1165/rcmb.2015-0055OC.

[124] R. Jones, M. Phil, L. Reid, Secretory cell hyperplasia and modification of intracellular glycoprotein in rat airways induced by short periods of exposure to tobacco smoke, and the effect of the antiinflammatory agent phenylmethyloxadiazole, Lab. Invest. 39 (1978) 41–49.

[125] R. Jones, P. Bolduc, L. Reid, Goblet cell glycoprotein and tracheal gland hypertrophy in rat airways: the effect of tobacco smoke with or without the anti-inflammatory agent phenylmethyloxadiazole, Br. J. Exp. Pathol. 54 (1973) 229–239. https://pubmed.ncbi.nlm.nih.gov/4121724.

[126] J.G. Heidsiek, D.M. Hyde, C.G. Plopper, J.A. St George, Quantitative histochemistry of mucosubstance in tracheal epithelium of the macaque monkey, J. Histochem. Cytochem. 35 (1987) 435–442, https://doi.org/10.1177/35.4.3819379.

[127] S. De Martin, D. Gabbia, S. Bogialli, F. Biasioli, A. Boschetti, R. Gstir, D. Rainer, L. Cappellin, Refill liquids for electronic cigarettes display peculiar toxicity on human endothelial cells, Toxicol. Reports. 8 (2021) 456–462, https://doi.org/10.1016/j.toxrep.2021.02.021.

[128] C.L. Gaworski, M.M. Dozier, S.R. Eldridge, R. Morrissey, N. Rajendran, J. M. Gerhart, Cigarette smoke vapor-phase effects in the rat upper respiratory tract, Inhal. Toxicol. 10 (1998) 857–873, https://doi.org/10.1080/089583798197420.